

Functionalized PAN based copolymer resins for adsorption of heavy metal ions

A Major Project Report

submitted in partial fulfilment of the requirements for the award of the degree

Of

MASTER OF TECHNOLOGY

IN

POLYMER TECHNOLOGY

Submitted by

ARUNA

(Roll No.: 2K12/PTE/03)

Under the esteemed guidance

Of

PROF. D. KUMAR



**Department of Applied Chemistry & Polymer Technology
Delhi Technological University
Main Bawana Road, Delhi-110042
July-2014**

**Department of Applied Chemistry & Polymer Technology
Delhi Technological University
Main Bawana Road, Delhi-110042**

CERTIFICATE

This is to certify that Ms. Aruna has carried out her major project II entitled “**Functionalized PAN based copolymer resins for adsorption of heavy metal ions**” under my supervision and guidance during the session 2013-14.

To the best of my knowledge and belief the content therein is her original work and has not been submitted to any other university or institution for the award of any degree or diploma.

Prof. D. Kumar
(Supervisor)
Head of the Department

STUDENT DECLARATION

I hereby declare that major project entitled “**Functionalized PAN based copolymer resins for adsorption of heavy metal ions**” is a record of original work done by me under the guidance of Prof. D. Kumar (Head of the Department), during the session 2013-14.

I also declare that no part of this report has been previously submitted to any University or any examining body for acquiring any degree.

ARUNA
(2K12/PTE/03)

ACKNOWLEDGEMENT

I wish to express my deep sense of gratitude and veneration to my project guide, Prof. D. Kumar, Head, Department of Applied Chemistry and Polymer Technology, Delhi Technological University, Delhi for his perpetual encouragement, constant guidance, valuable suggestions and continued motivation which has enabled me to complete this project work.

I am deeply indebted to Dr. Roli Purwar, Dr. G .L. Verma, Dr. A. P. Gupta, Dr. R. C. Sharma, Dr. D. Santhiya, Dr. Ram Singh, Dr. Anil Kumar, Dr. Richa Srivastava, Dr. Raminder Kaur, Shri S. G. Warker and Dr. Archana Rani for their constant guidance and facilities to carry out my project work.

I would like to continue by thanking Ms. Sarita, Ms. Reetu (research scholars), Mr. A. V. Ullas, Mr. Sandeep Mishra and Mr. Aman Verma (Technical assistant) for their massive help in making me understand the basics of techniques and patiently responding to my incessant doubts.

I am thankful to all laboratory staff and colleagues for their co-operation.

Lastly, I wish to thank my friends Navneet Kumar and Chansi for their motivation and cooperation all throughout.

Aruna

(Roll No- 2K12/PTE/03)

INDEX

CONTENT	PAGE NO.
➤ LIST OF FIGURES AND TABLES	
➤ CODING AND ABBREVIATIONS	
➤ ABSTRACT	
➤ OBJECTIVE	
 ➤ CHAPTER 1 INTRODUCTION	
➤ CHAPTER 2 LITERATURE REVIEW	
2.1 Homopolymer: PAN and others	
2.2 PAN based composites and other copolymers	
 ➤ CHAPTER 3 EXPERIMENTAL	
3.1 Materials	
3.2 Methods	
3.2.1 Synthesis of polyacrylonitrile	
3.2.2 Synthesis of poly(acrylonitrile-styrene) copolymer	
3.2.3 Synthesis of poly(acrylonitrile-acrylamide) copolymer	
3.2.4 Synthesis of poly(acrylonitrile-methacrylic acid) Copolymer	
3.2.5 Synthesis of functionalized PAN based copolymer resins	
3.2.6 Functionalization method	
3.2.7 Sorption of metal ions	
3.2.8 Molecular weight determination	

3.3 Characterization

3.3.1 Fourier Transform Infrared Spectroscopy

3.3.2 Energy-Dispersive X-ray Spectroscopy

3.4 Analysis

3.4.1 Scanning Electron Microscopy

3.4.2 Thermogravimetric Analysis

3.4.3 Differential Scanning Colorimeter

3.4.4 Dynamic Mechanical Analysis

➤ CHAPTER 4 RESULTS AND DISCUSSION

4.1 Molecular weight determination

4.2 FTIR Analysis

4.3 EDS Analysis

4.4 SEM Analysis

4.5 TGA

4.6 DSC Analysis

4.7 DMA

➤ CHAPTER 5 CONCLUSION

➤ CHAPTER 6 FUTURE PROPECTUS

➤ REFERENCES

LIST OF FIGURES AND TABLES

CONTENT

Fig. 1.1: General structure of polyacrylonitrile

Fig. 1.2: General structure of polystyrene

Fig. 1.3: General structure polyacrylamide

Fig. 1.7: General structure of polymethacrylic acid

Fig. 1.9: General structure of triethylenetetramine

Fig. 2.1: SEM micrographs of functionalized PAN resins (a) after adsorption of Hg (b after adsorption of Fe

Fig. 2.2: Effect of acidity on the sorption of PAN based resin for Rh(III), Ru(IV), Ir(IV) and Pd(II)

Fig. 2.3: Probable chemical structure of the polybenzoxazine aerogel

Fig. 2.4: FTIR spectra of polyacrylonitrile–Ethylenediamine at different time periods for 70 °C

Fig. 2.5: SEM micrograph of the cross section of the PAN support (a) top layer (b) bottom layer

Fig. 2.6: Infrared spectra of neat SiO₂, SiO₂ 20%/APTES 50%, Neat PAN, PAN/SiO₂ 20% and PAN/SiO₂ 20%/APTES 50%

Fig. 2.7: Metal adsorption (mmol/g) at different pH for adsorbent P(NPDA-AAg).; Contact time: 1 h; Resin/metal ion ratio: 20:1 (mmol base), Temp: 20 °C

Fig. 3.1: Schematic diagram of Ostwald Viscometer

Fig. 3.2: Plot of η_{sp}/C or η_r/C versus C for PAN in DMF at 30°C

Fig. 3.3: Plot of η_{sp}/C or η_r/C versus C for PANS copolymer in DMF at 30°C

Fig. 3.4: Plot of η_{sp}/C or η_r/C versus C for PANAm copolymer in DMF at 30°C

Fig. 3.5: Plot of η_{sp}/C or η_r/C versus C for PANMA copolymer in DMF at 30°C

Fig. 3.6: Nicolet 380 Fourier Transform Infrared Spectrometer

Fig. 3.7: Hitachi Hi Technologies S_3700 N Scanning Electron Microscope

Fig. 3.8: TA instruments Thermogravimetric analyzer Q 50

Fig. 3.9: Perkin Elmer Dynamic Mechanical Analyzer DMA 8000

Fig. 3.10: TA Instruments DSC Q20

Fig. 4.1: FTIR spectra of PAN resin

Fig. 4.2: FTIR spectra of PANS copolymer resin

Fig. 4.3: FTIR spectra of PANAm copolymer resin

Fig. 4.4: FTIR spectra of PANMA copolymer resin

Fig. 4.5: FTIR spectra of functionalized PAN resin

Fig. 4.6: FTIR spectra of functionalized PANS resin

Fig. 4.7: FTIR spectra of functionalized PANAm resin

Fig. 4.8: FTIR spectra of functionalized PANMA resin

Fig. 4.9: EDS graph of F1-PAN for the absorption of Fe^{2+}

Fig. 4.10: EDS graph of F1-PAN for the absorption of Hg^{2+}

Fig. 4.11: EDS graph of F1-PANS for the absorption of Fe^{2+}

Fig. 4.12: EDS graph of F1-PANS for the absorption of Hg^{2+}

Fig. 4.13: EDS graph of F1-PANAm for the absorption of Fe^{2+}

Fig. 4.14: EDS graph of F1-PANAm for the absorption of Hg^{2+}

Fig. 4.15: EDS graph of F1-PANMA for the absorption of Fe^{2+}

Fig. 4.16: EDS graph of F1-PANMA for the absorption of Hg^{2+}

Fig. 4.17: EDS graph of F2-PAN for the absorption of Fe^{2+}

Fig. 4.18: EDS graph of F2-PAN for the absorption of Hg^{2+}

Fig. 4.19: EDS graph of F2-PANS for the absorption of Fe^{2+}

Fig. 4.20: EDS graph of F2-PANS for the absorption of Hg^{2+}

Fig. 4.21: EDS graph of F2-PANAm for the absorption of Fe^{2+}

Fig. 4.22: EDS graph of F2-PANAm for the absorption of Hg^{2+}

Fig. 4.23: EDS graph of F2-PANMA for the absorption of Fe^{2+}

Fig. 4.24: EDS graph of F2-PANMA for the absorption of Hg^{2+}

Fig. 4.25: Graphical representation of wt. % of Hg^{2+} and Fe^{2+} absorbed by functionalized resins

Fig. 4.26: SEM micrograph of F1-PAN

Fig. 4.27: SEM micrograph of F1-PANS

Fig. 4.28: SEM micrograph of F1-PANAm

Fig. 4.29: SEM micrograph of F1-PANMA

Fig. 4.30: SEM micrograph of F2-PAN

Fig. 4.31: SEM micrograph of F2-PANS

Fig. 4.32: SEM micrograph of F2-PANAm

Fig. 4.33: SEM micrograph of F2-PANMA

Fig. 4.34: TGA thermogram of F2-PAN

Fig. 4.35: TGA thermogram of F2-PANS

Fig. 4.36: TGA thermogram of F2-PANAm

Fig. 4.37: TGA thermogram of F2-PANMA

Fig. 4.38: Heat flow v/s Temperature graph of F2-PAN

Fig. 4.39: Heat flow v/s Temperature graph of F2-PANS

Fig. 4.40: Heat flow v/s Temperature graph of F2-PANAm

Fig. 4.41: Heat flow v/s Temperature graph of F2-PANMA

Fig. 4.42: Dynamic properties v/s Temperature graph of F2-PAN

Fig. 4.43: Dynamic properties v/s Temperature graph of F2-PANS

Fig. 4.44: Dynamic properties v/s Temperature graph of F2-PANAm

Fig. 4.45: Dynamic properties v/s Temperature graph of F2-PANMA

Table 3.1: Functionalization composition of PAN and its copolymers

Table 3.2: Viscosity data for PAN in DMF at 30°C

Table 3.3: Viscosity data for PANS in DMF at 30°C

Table 3.4: Viscosity data for PANAm in DMF at 30°C

Table 3.5: Viscosity data for PANMA in DMF at 30°C

Table 4.1: Molecular weight and viscosity measurement data of the samples

Table 4.2: Wt. % adsorption for Hg^{2+} and Fe^{2+} of various polymer resins

CODING AND ABBREVIATIONS

1.	TETA	Triethylenetetramine
2.	F1	Functionalization with resin and TETA in 1:10 ratio
3.	F1-PAN	Functionalized polyacrylonitrile resin
4.	F1-PANS	Functionalized poly(acrylonitrile-styrene) resin
5.	F1-PANAm	Functionalized poly(acrylonitrile-acrylamide) resin
6.	F2-PANMA	Functionalized poly(acrylonitrile-methacrylic acid) resin
7.	F2	Functionalization with resin and TETA in 1:15 ratio
8.	F2-PAN	Functionalized polyacrylonitrile resin
9.	F2-PANS	Functionalized poly(acrylonitrile-styrene) resin
10.	F2-PANAm	Functionalized poly(acrylonitrile-acrylamide) resin
11.	F2-PANMA	Functionalized poly(acrylonitrile-methacrylic acid) resin

ABSTRACT

In this report functionalized polyacrylonitrile (PAN) based copolymer resins were synthesized which can act as adsorbent for the adsorption of heavy metal/metal ions like Fe^{2+} and Hg^{2+} etc. Firstly, PAN and its copolymers were synthesized using styrene, acrylamide and methacrylic acid comonomers. PAN and its copolymers like poly(acrylonitrile-styrene) [PANS], poly(acrylonitrile-acrylamide) [PANAm], and poly(acrylonitrile-methacrylic acid) [PANMA] were functionalized using different concentration of triethylenetetramine (TETA) to obtain two series of polymer resins such as F1-PAN, F1-PANS, F1-PANAm, F1-PANMA, F2-PAN, F2-PANS, F2-PANAm and F2-PANMA, where F1 and F2 represents 1:10 and 1:15 resin to TETA ratio, respectively. These resins have been characterized by using Fourier Transform Infrared Spectroscopy (FTIR) and Energy Dispersive X-Ray Spectroscopy (EDS) techniques. Thermal characterization of resins was performed by Differential Scanning Colorimeter (DSC), Thermogravimetric Analysis (TGA) and Dynamic Mechanical Analysis (DMA). The surface morphology was studied by using Scanning Electron Microscopy (SEM) and viscosity average molecular weight was also determined by viscometric method. The appearance of C=O, C=NH and C=N groups on functionalization of resins was confirmed by FTIR data. EDS study show that F2-PANS and F2-PANMA possess highest adsorption capacity for Hg^{2+} and Fe^{2+} metal ions. The TGA technique was used to study the effect of copolymerization and functionalization on copolymers and it was found that there is no adverse effect of copolymerization and functionalization on the thermal stability of the resins. The SEM results also support the EDS results and show the presence of a large number of pores in F2-PANS and F2-PANMA which was probably responsible for their higher adsorption capacity. DMA studies reveal that Glass transition temperature (T_g) of F2-PANMA is highest, i.e., 106.8 °C. The DSC results also support the DMA data. The calculated viscosity average molecular weight for PAN and its copolymers poly(acrylonitrile-styrene), poly(acrylonitrile-acrylamide) and poly(acrylonitrile-methacrylic acid) is found to be 130606, 150304, 157022 and 167233, respectively.

OBJECTIVE

The main objective of this project work is to synthesize functionalized PAN and functionalized PAN based copolymer resins for the adsorption of heavy metal/metal ions from aqueous solution. Copolymers of acrylonitrile have been synthesized by using comonomers such as styrene, acrylamide and methacrylic acid by free radical polymerization using benzoyl peroxide as an initiator. These copolymers have been functionalized by using different concentrations of triethylenetetramine reagent. Eight samples; F1-PAN, F1-PANS, F1-PANAm, F1-PANMA, F2-PAN, F2-PANS, F2-PANAm and F2-PANMA have been synthesized. These resins have been used as an adsorbent for the sorption of metal ions such as Hg^{2+} and Fe^{2+} from aqueous solution. Sorption behaviour of resins has also been studied and the detection of heavy metal/metal ions was carried out by using EDS technique. Characterization of functionalized PAN based resins was carried out by FTIR and SEM technique was used to study the morphology of resins. Further, DSC, TGA and DMA techniques were used to determine the thermal properties of the resins. Molecular weight of polymers and copolymers was also determined in the present work.

CHAPTER-1

INTRODUCTION

Many chemical and industrial processes are responsible for the water pollution and environmental contaminations. Since, waste water contains a large amount of heavy metals; therefore removal of these metals from the water is the prime interest of this work. Metal ions are being used widespread in many industrial processes and applications which causes serious environmental problems. Among these industrial effluents are catalysts, magnets, gear, industrial fertilizer, airbag valves, tooth protects, electronics, etc. In order to resolve these problems, different materials such as ion exchange resins and fibres have been used. In recent years, the utilization of chelate sorbents in forming strong complexes with heavy metal/metal ions has been considered. Many different synthetic materials with complexation or chelation properties have been prepared for the application in industrial plants and chemical processes. In PAN and PAN based copolymers active nitrile groups present allow introducing new functional groups by chemical reactions^[1]. Different methods have been reported for the surface modification of PAN and its copolymers. These PAN copolymers based resins are convenient for waste water treatment applications. They are able to adsorb various impurities very fast due to their chelation or complexation abilities through their reactive groups, such as amine, nitrile, amide, carboxylic acid, etc.

PAN is a synthetic, semi-crystalline organic polymer resin, with the linear formula $(C_3H_3N)_n$. Though, it is thermoplastic, it does not melt under normal conditions and it degrades before melting. It melts above 300°C, if the heating rate is 50 °C/min or above^[2]. Almost all polyacrylonitrile resins are copolymers made from mixtures of monomers with acrylonitrile as the main component. It is a versatile polymer used to produce large variety of products including ultra-filtration membranes, hollow fibers for reverse osmosis, fibers for textiles and oxidized PAN fibers. PAN fibers are the chemical precursor of high-quality carbon fiber. PAN is first thermally oxidized in air at 230°C to form an oxidized PAN fiber and then carbonized above 1000°C in inert atmosphere to make carbon fibers found in plenty of both high-tech and common daily applications such as civil and military aircraft primary and secondary structures, missiles, solid propellant rocket motors, pressure vessels, fishing rods, tennis rackets, badminton rackets and high-tech bicycles. It is a component repeat unit in several important copolymers, such as styrene-acrylonitrile (SAN) and acrylonitrile butadiene styrene (ABS) plastic. PAN resin is a rigid, hard thermoplastic material, resistant to most of the chemicals and solvents. Most of

the PAN is produced as acrylic fibre is a common substitute for wool in clothing. The acrylonitrile repeating unit of the polymer has the following structure (fig. 1.1):

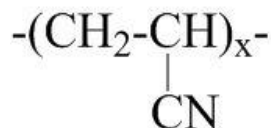


Fig. 1.1: General structure of polyacrylonitrile

Polyacrylonitrile is a synthetic resin, can be prepared by the free radical polymerization of acrylonitrile. Acrylonitrile is synthesized by reacting propylene with ammonia and oxygen in the presence of catalyst. Acrylonitrile monomers (single-unit molecules) are suspended, almost always in combination with other monomers, as fine droplets in water and are induced to polymerize to PAN through the action of free-radical initiators.

PAN has none of the hazardous properties of the monomer. Owing to the formation of strong chemical bonds between the nitrile (-CN) groups, the polymer molecules resist most organic solvents and do not melt without decomposing. In most cases the polymer is dissolved in special solvents and spun into acrylic fibres, which are defined as fibres that contain 85 % or more of PAN. Because PAN is difficult to dissolve and is highly resistant to dyeing, very little fibre is produced containing PAN alone. PAN has various properties such as good thermal stability, high strength, modulus of elasticity and low density. PAN has ability to absorb many metal ions, which makes it important for the application in adsorption processes^[3].

Physical properties of PAN:

Glass transition temperature (T_g): $\sim 95^\circ\text{C}$.

Solubility parameters: $26.09 \text{ MPa}^{1/2}$ (25°C)

Density: 1.15 gcm^{-3} .

Polystyrene (fig. 1.2) is a hard, stiff and brilliantly transparent synthetic resin produced by the polymerization of styrene. It is widely employed in the food-service industry as rigid trays and containers, disposable eating utensils, foamed cups, plates and bowls. Polystyrene is also copolymerized or blended with other polymers, lending hardness and rigidity to a number of important plastic and rubber products. Styrene is obtained by reacting ethylene with benzene in the presence of aluminium chloride (AlCl_3) to yield ethylbenzene. The benzene group in this compound is then dehydrogenated to yield phenylethylene or styrene a clear liquid hydrocarbon with the chemical structure $\text{CH}_2=\text{CHC}_6\text{H}_5$. Styrene is polymerized by using free-radical initiators

primarily in bulk and suspension processes, although solution and emulsion methods are also employed. The presence of the pendant phenyl (C_6H_5) groups is a key to the properties of polystyrene. Solid polystyrene is transparent, owing to these large, ring-shaped molecular groups, which prevent the polymer chains from packing into close, crystalline arrangements^[5]. In addition, the phenyl rings restrict rotation of the chains around the C-C bonds, lending the polymer its noted rigidity.

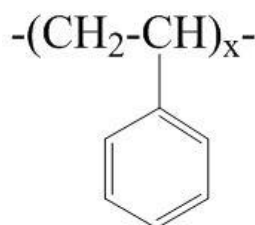


Fig. 1.2: General structure of polystyrene

The polymerization of styrene has been known since 1839, when German pharmacist Eduard Simon reported its conversion into a solid later named meta-styrol. As late as 1930, little commercial use had been found for the polymer because of brittleness and crazing (minute cracking), which were caused by impurities that brought about the cross-linking of the polymer chains^[4].

Polyacrylamide (fig. 1.3) is prepared from acrylamide monomer by free radical polymerisation using benzoyl peroxide as a catalyst. Polyacrylamide is not toxic in nature and in cross-linked form possibility of the monomer being present is reduced. It has high water adsorbent property and forming soft gel when hydrated. It is used in many applications such as polyacrylamide gel electrophoresis and in contact lenses. Recently, polyacrylamide is being largely used to flocculate solids in a liquid; process applies to water treatment and paper making. Another common use of polyacrylamide and its derivatives is in subsurface applications such as enhanced oil recovery (EOR). High viscosity aqueous solutions can be generated with low concentrations of polyacrylamide polymers, and these can be injected to improve the economics of conventional water flooding. Cross-linked polyacrylamide in anionic form is most frequently used as a soil conditioner on construction sites and farm lands for the erosion control to maintain the water quality. Ionic form of polyacrylamide is very useful in the treatment of portable water of industry. Aluminium chloride and Ferric chloride are trivalent metal salts, can be bridged by the long polymer chains of polyacrylamide^[4].

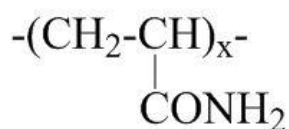


Fig. 1.3: General structure of polyacrylamide

Poly methacrylic acid (fig. 1.4) was prepared by polymerizing the methacrylic acid monomer. It is also found as salt of metals.

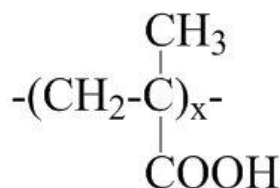


Fig. 1.4: General structure of polymethacrylic acid

Triethylenetetramine (fig. 1.5) is an organic compound with molecular formula $[\text{NH}_2\text{CH}_2\text{CH}_2\text{NH}_2\text{CH}_2\text{CH}_2\text{NH}_2\text{CH}_2\text{CH}_2\text{NH}_2]$. It is also abbreviated as TETA and triene. This is oily liquid and colourless but sometime like many amines it is found as yellowish in colour due to oxidation by air. Triethylenetetramine is synthesized by the reaction of ethylenediamine and ammonia mixture over an oxide catalyst. Many varieties of amines have been prepared by this process, which are separated by distillation and separation processes.

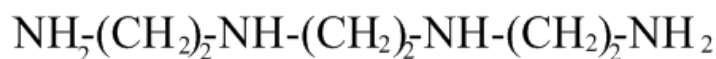


Fig. 1.5: General structure of triethylenetetramine

Triethylenetetramine was primarily used as a cross-linker for the hardening or curing of epoxy resin. Trientine hydrochloride used as a chelating agent is a hydrochloride salt of triethylenetetramine. This trientine hydrochloride is used to bind up and remove Cu (Copper) in the body to treat Wilson's disease, particularly in those who are intolerant to penicillamine. Triethylenetetramine is also called a tetra dentate ligand in co-ordination chemistry because it can donate four lone pair of electrons to the metal ion. It forms chelating complexes with metal atom or ion^[6]. Because of its chelating property it has been used in this project work for functionalization of PAN and PAN based copolymer resins.

CHAPTER-2

LITERATURE REVIEW

PAN has a wide range of applications in many areas including biomedical and textile industries etc. Its crystallinity imparts some special characteristics. In literature, a large number of PAN copolymers are present with varieties of applications. Homopolymers of PAN have been used as fibers in hot gas filtration systems, outdoor awnings, sails for yachts and even fiber reinforced concrete but mostly copolymers containing PAN are used as fibers to make knitted clothing, like socks and sweaters, as well as outdoor products like tents. Some of the famous examples of copolymers are ABS [poly (acrylonitrile-butadiene-styrene)] and NBR (nitrile rubber). These are famous for their mechanical properties. Now, researchers are keen interested to exploit its other properties. PAN and its copolymers are being developed as adsorbent.

2.1 Homopolymers: PAN and others

G.R. Kiani, H. Sheikhloie and N. Arsalani synthesized PAN and functionalized it for the removal of heavy metals from aqueous solution. They investigated the adsorption of Zn(II), Ag(I), Fe(III), Pb(II) and Hg(II) from aqueous solutions utilizing functionalized polyacrylonitrile adsorbent^[7]. They functionalized PAN by reacting with diethylenetriamine (DTA) to obtain amine containing resin that can adsorb heavy metals from aqueous solution. The resins and its metal complexes were studied by TGA and FTIR techniques. In order to study the surface morphologies SEM was utilized. SEM micrographs (fig. 2.1) show that there is a little change in the morphology of resins after the adsorption.

Amounts of adsorption depend on the amine content of the functionalized resins and increase of amine content in resins, resulted in metal ion adsorption increment. It is obvious because as the amine content increases the number of reactive sites also increases which resulted in an increase in the amount of adsorption of heavy metals.

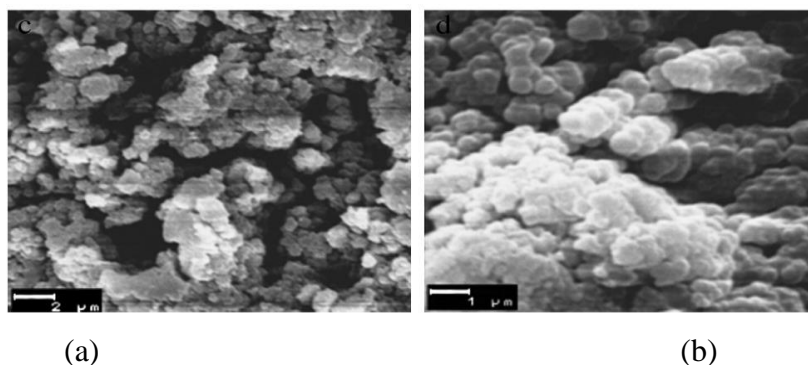


Fig. 2.1: SEM micrographs of functionalized PAN resins (a) after adsorption of Hg and (b) after adsorption of Fe

Yiyong Chen and Yan Zhao synthesized and characterized PAN based resin (polyacrylonitrile-2-amino-2-thiazoline) and studied its sorption behaviours for noble metal ions^[8]. Polyacrylonitrile-2-amino-2-thiazoline resin was synthesized from cross-linked polyacrylonitrile and 2-amino-2-thiazoline. The structure of PAN based resin was confirmed by X-ray photoelectron spectroscopy (XPS) and elemental analysis. The effect of acidic medium on the sorption of PAN based resins was also studied (fig. 2.2).

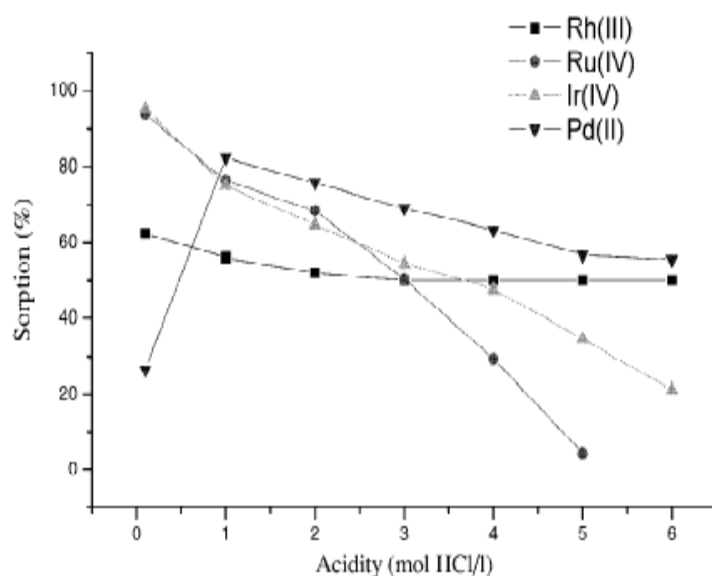


Fig. 2.2: Effect of acidity on the sorption of PAN based resin for Rh(III), Ru(IV), Ir(IV) and Pd(II)

The results show that the sorption of Pd(II) and Rh(III) was high over a wide range of acidity. The percentage conversion of functional group and functional group capacity of PAN based resin synthesized under the optimum condition were 15.90% and 2.002 mmol/g, respectively. They studied the sorption behaviour of PAN based resin for Ru(IV), Ir(IV), Rh(III) and Pd(II).

Thanyalak Chaisuwan et al investigated the removal of heavy metals from model waste water by using polybenzoxazine resin. They used polybenzoxazine aerogel as a chelating polymer. The following order of removal of heavy metal ions was deduced from the results: $\text{Sn}^{2+} > \text{Cu}^{2+} > \text{Fe}^{2+} > \text{Pb}^{2+} > \text{Ni}^{2+} > \text{Cd}^{2+} > \text{Cr}^{2+}$, which was found in accordance with the Irving–Williams rule^[9]. Also, the amount of metal ions removed depended on the sorption time and the amount of absorbent. It was found that the desorption process was a function of temperature, pH and type of solution. The proposed structure of polybenzoxazine aerogel (fig. 2.3) is given below.

The effect of time was studied by the FTIR of PAN-EDA at 70°C for different time intervals ranging from 4 to 24 h. Many significant changes is observed from FTIR of PAN-EDA. With increase in the time the intensity of the adsorption band of the nitrile group stretching at 1252 and 2243 cm^{-1} and bending at 1075 cm^{-1} decreases, while the broad band at 3407 cm^{-1} attributed to the stretching vibration of the –NH groups is also increased (Fig. 2.4).

2.2 PAN based composites and other copolymers:

Chalida Klaysom et al investigated the characterization, performance evaluation and film optimization of Polyamide/Polyacrylonitrile thin film composite as osmosis membranes^[11]. Reaction time composition of the reaction mixture and air drying period were the selected properties for the optimization by fine tuning preparation in interfacial polymerisation. The key parameters found to have a significant effect on the selective layer properties were the drying period of the excess amine solution on the support surface before contacting with the second reagent and the surfactant additive. The SEM images of the cross section of the PAN support is shown below (fig. 2.5).

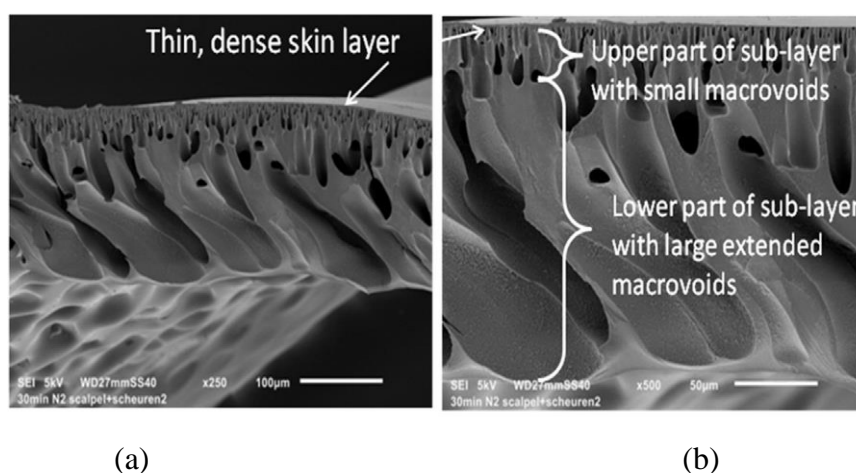


Fig. 2.5: SEM micrographs of the cross section of the PAN support (a) top layer (b) bottom layer

The finger-like pore structures with a dense top layer and a more porous bottom layer were visible. The thickness of the support measured was around 160 ± 10 μm. It can be deduced from the above SEM micrographs that prepared support was highly porous and asymmetric.

Adsorption of Cd^{2+} , Th^{4+} , Ni^{2+} and U^{6+} using modified polyacrylonitrile composite nanofiber adsorbent was investigated by Abolfazl Dastbaza, Ali Reza and Keshtkarb. Synthesis of adsorbent was carried out by using electro-spinning process^[12]. SiO_2 nanoparticles were selected

as reinforcement and modified by 3-aminopropyltriethoxysilane (APTES) and then applied by electrospinning process to develop a polyacrylonitrile composite nanofibre adsorbent. FTIR, BET (Brunauer-Emmett-Teller)) and SEM analysis were carried out for the characterization of composite. Also the influence of SiO₂, APTES and pH on the properties of polyacrylonitrile composite nanofiber adsorbent was studied.

The FTIR results confirmed the presence of SiO₂ and SiO₂/APTES nanoparticles in PAN nanofiber, PAN/SiO₂ and PAN/SiO₂/APTES composite nanofibers. In the FTIR spectra (fig. 2.6) of SiO₂ and SiO₂/APTES, the adsorption peak at 1020–1200 cm⁻¹ was due to the Si-O-Si asymmetric stretch.

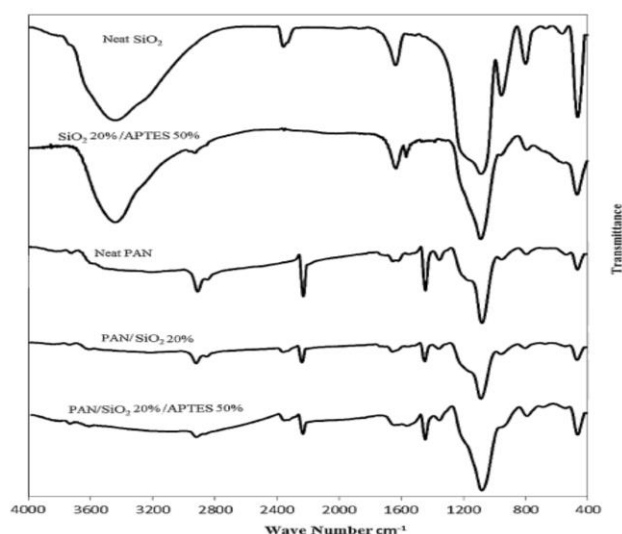


Fig. 2.6: Infrared spectra of neat SiO₂, SiO₂ 20%/APTES 50%, Neat PAN, PAN/SiO₂ 20% and PAN/SiO₂ 20%/APTES 50%

The modified SiO₂ spectra show that the adsorption band around 1570 cm⁻¹ could be assigned to the stretching vibrations of secondary amine (N-H). The adsorption peak at 2240 cm⁻¹ is the vibration band of the nitrile group (C-N) as shown in the spectra of PAN, PAN/SiO₂ and PAN/SiO₂/APTES. The results show that the optimum content of APTES and SiO₂ are 50% and 20%, respectively. For the adsorption of U⁶⁺, Cd²⁺, Th⁴⁺ and Ni²⁺ the optimum pH found was 5, 6, 4 and 6, respectively.

Attention was also given to the environmental impacts on adsorbent used to remove the heavy metals. Bernabe et al synthesized a novel adsorbent for heavy metal adsorption and studied the effect of environmental factors on the properties of adsorbent. Poly(N-(3-dimethylamino)propylmethacrylamide-co-4-acryloylmorpholine) [P(NDAPA-AMo)], poly(N-(3-dimethylamino)propylmethacrylamide-co-2-acrylamidoglycolic acid) [P(NDAPA-AAg)] and

poly(N-(3-dimethylamino)propylmethacrylamide-co-acrylic acid) [P(NDAPA-AA)] were synthesized by free radical polymerisation. Hg^{2+} , Cr^{3+} , Pb^{2+} , Cd^{2+} and Zn^{2+} were the metals selected for this study^[13]. Their adsorption was studied with respect to initial metal ion concentration, initial pH and temperature using batch-equilibrium technique. Acid and basic regeneration was tested to restore the adsorbent to initial conditions.

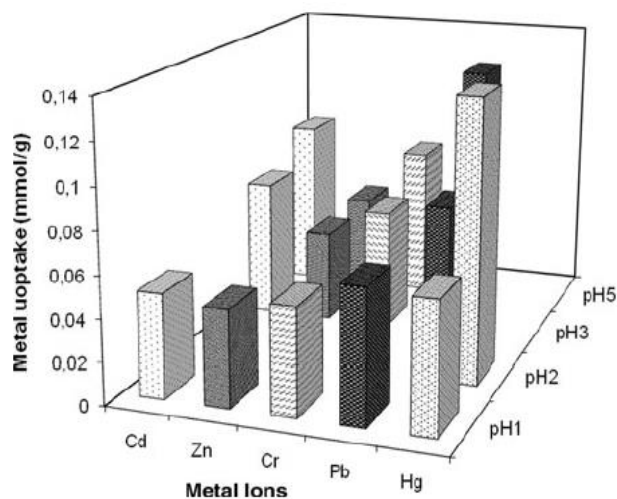
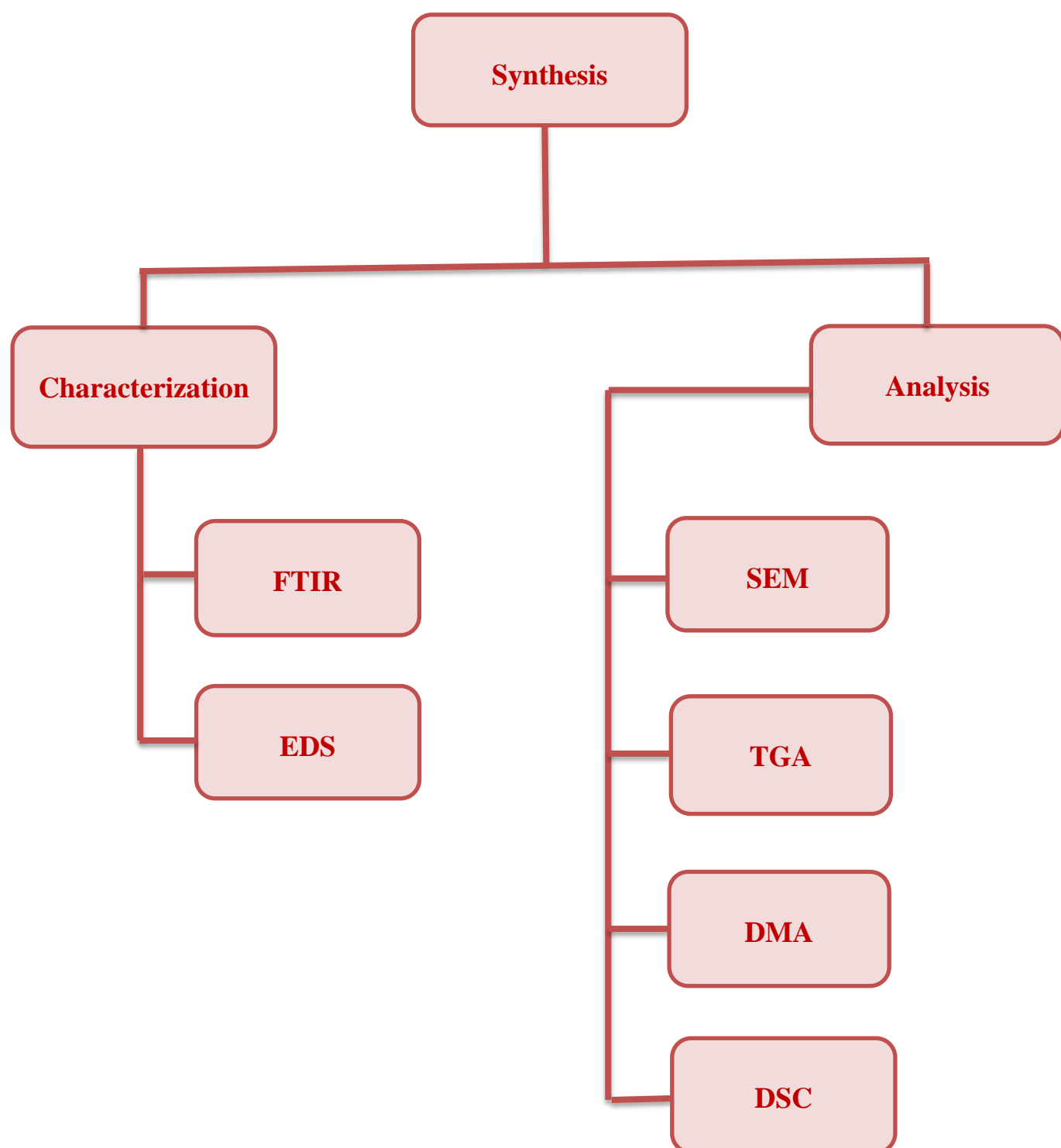


Fig. 2.7: Metal adsorption (mmol/g) at different pH for adsorbent P(NPDA-AAg);
Contact time: 1 h; Resin/metal ion ratio: 20:1 (mmol base) Temp: 20 °C

As shown above (Fig. 2.7), Hg^{2+} shows higher retention at pH 2. This is probably due to increase in availability of carboxylate groups at lower pH. Other polymers show higher retention at higher pH. P(NDAPA-co-AAg) resin shows the higher retention of Hg^{2+} while other resins P(NDAPA-AA) and P(NDAPA-AMo) show an improved ability to retain Cr^{3+} .

From the literature survey, it is found that the main problem with these resins, they could not retain a large amount of heavy metal/metal ions and functional groups are responsible for the adsorption. So we can say that the insertion of functional groups can increase the adsorption capacity of resin upto a greater extent. Hence, the main objective of this project work is to increase the chelating effect of the resin by functionalization so that resin can adsorb a large amount of heavy metal/metal ions from aqueous solution. To perform the functionalization process or to enhance the chelating effect, chelating agent such as TETA is used as a functionalizing agent.

Work Plan



CHAPTER-3

EXPERIMENTAL

3.1 Materials

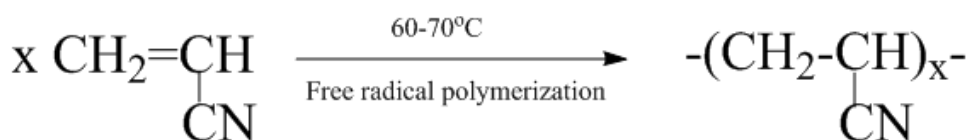
Following materials/chemicals were taken to perform the experiments:

Acrylonitrile, styrene, acrylamide, methacrylic acid, benzoyl peroxide, potassium persulphate and triethylenetetramine have been used in the present work. All the above mentioned chemicals were purchased from Central Drug House, Delhi.

3.2 Methods

3.2.1 Synthesis of polyacrylonitrile:

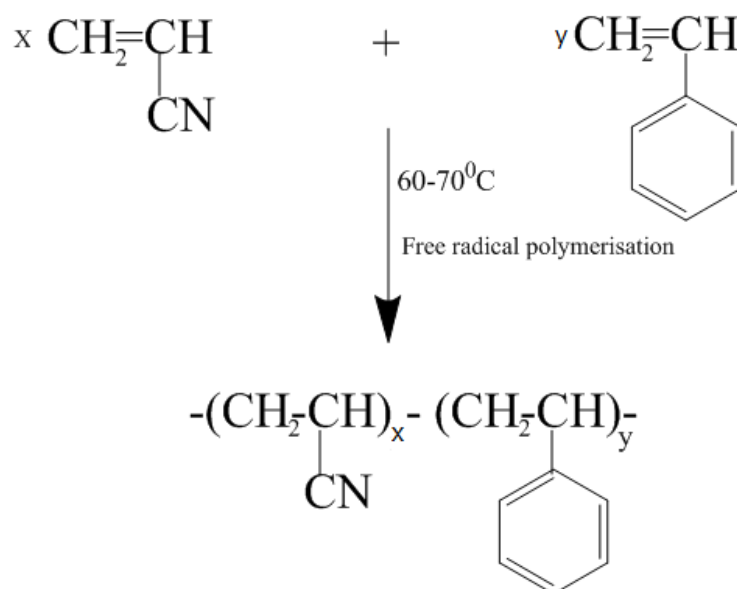
Polyacrylonitrile was synthesized using free radical polymerization (scheme 3.1) by adding 60 mL of acrylonitrile monomer, 0.2 g of potassium persulphate as a catalyst, 0.2 g of benzoyl peroxide as an initiator in 100 mL of distilled water. The contents were heated in a conical flask at 60 °C in water bath for 1h. The mixture precipitated out after 1 h and then precipitate was filtered, washed and dried in oven.



Scheme 3.1: Synthesis of polyacrylonitrile from acrylonitrile

3.2.2 Synthesis of poly(acrylonitrile-styrene) copolymer:

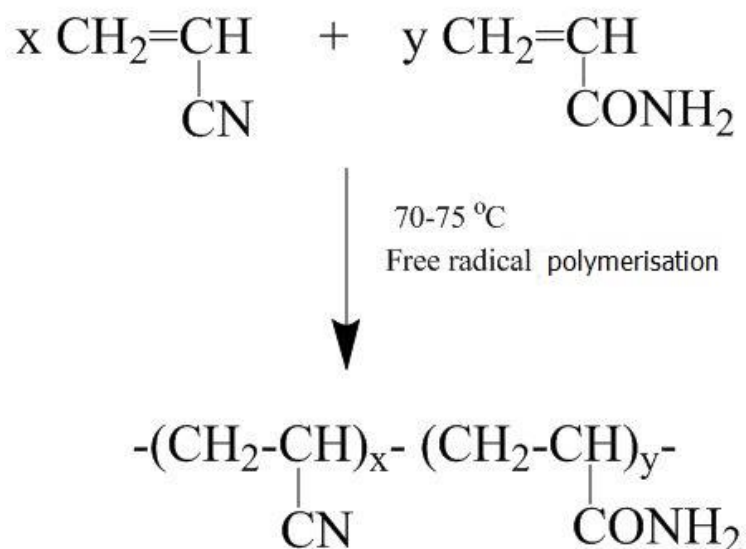
Copolymer of acrylonitrile-styrene was synthesized by copolymerization (scheme 3.2) of 90 mL of acrylonitrile with 10 mL of styrene in the presence of 0.3 g potassium persulphate, 0.3 g benzoyl peroxide and 100 mL of water in a conical flask and heated at 60-70 °C in water bath for 2 h. The mixture precipitated out after 2 h and then precipitate was filtered, washed and dried in oven.



Scheme 3.2: Synthesis of poly(acrylonitrile-styrene) copolymer

3.2.3 Synthesis of poly(acrylonitrile-acrylamide) copolymer:

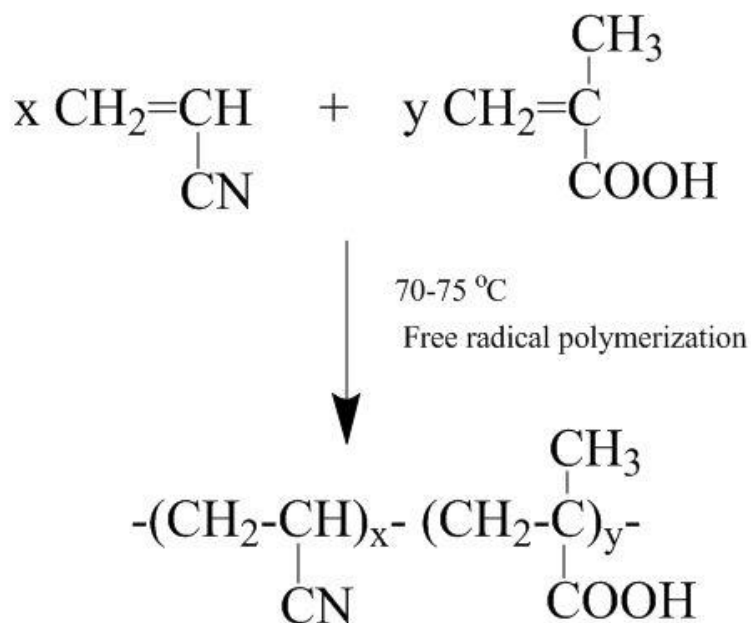
Copolymer of acrylonitrile-acrylamide was synthesized by copolymerization (scheme 3.3) of 50 mL of acrylonitrile with 6.6 g of acrylamide in the presence of 0.2 g potassium persulphate, 0.2 g benzoyl peroxide and 100 mL of water in a conical flask and heated at 60-70 °C in water bath for 1.5 h. The mixture precipitated out after 1 h and then precipitate was filtered, washed and dried in oven.



Scheme 3.3: Synthesis of poly(acrylonitrile-acrylamide) copolymer

3.2.4 Synthesis of poly(acrylonitrile-methacrylic acid) copolymer:

Copolymer of acrylonitrile-methacrylic acid was synthesized by copolymerization (scheme 3.4) of 50 mL of acrylonitrile with 6 mL of methacrylic acid in the presence of 0.2 g potassium persulphate, 0.2 g benzoyl peroxide and 100 mL of water in a conical flask and heated at 60-70 °C in water bath for 1.5 h. The mixture precipitated out after 1.5 h and then precipitate was filtered, washed and dried in oven.



Scheme 3.4: Synthesis of poly(acrylonitrile-methacrylic acid) copolymer

3.2.5 Synthesis of functionalized PAN based copolymer resins:

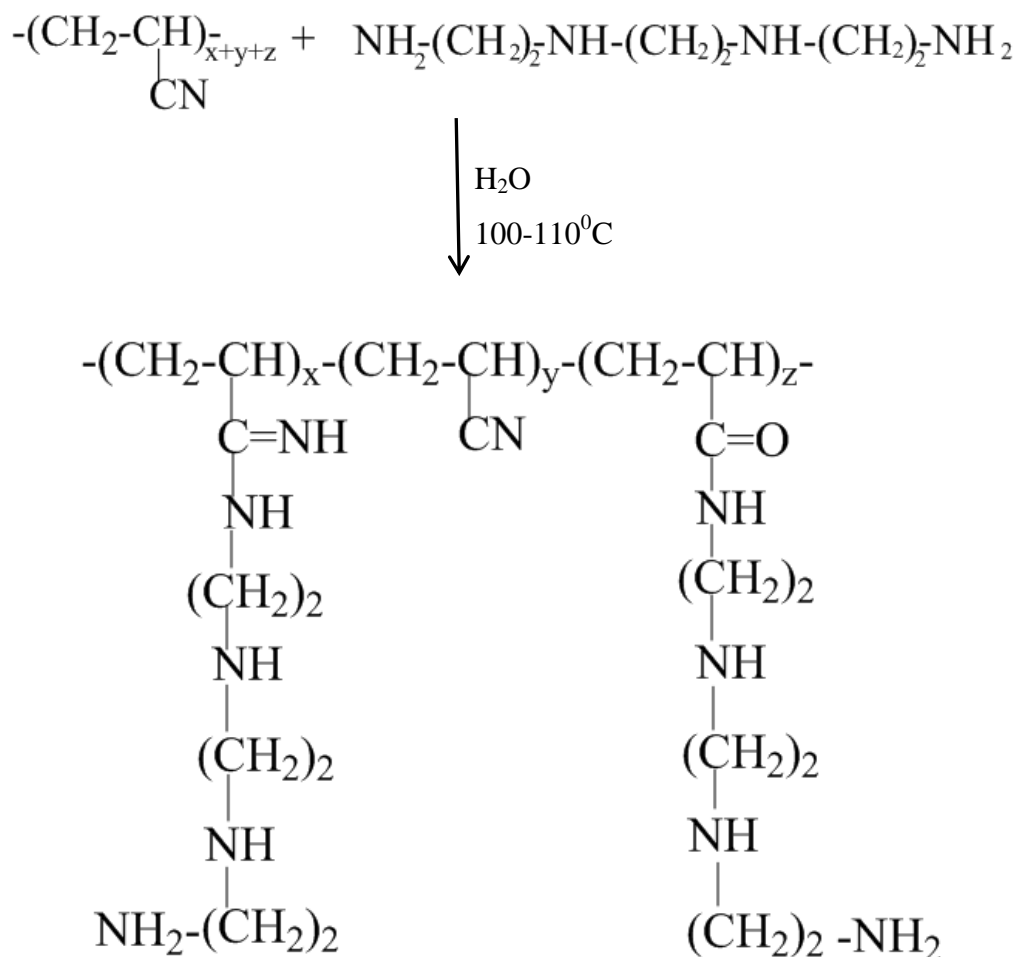
Eight samples of functionalized PAN and its copolymer based resins have been synthesized to obtain two series F1 and F2; F1-PAN, F1-PANS, F1-PANAm, F1-PANMA, F2-PAN, F2-PANS, F1-PANAm and F2-PANMA. Functionalization process of resins was carried out by using two types of composition having different ratios of resin and triethylenetetramine and data so obtained is presented in table 3.1.

Table 3.1: Functionalization composition of PAN and its copolymers

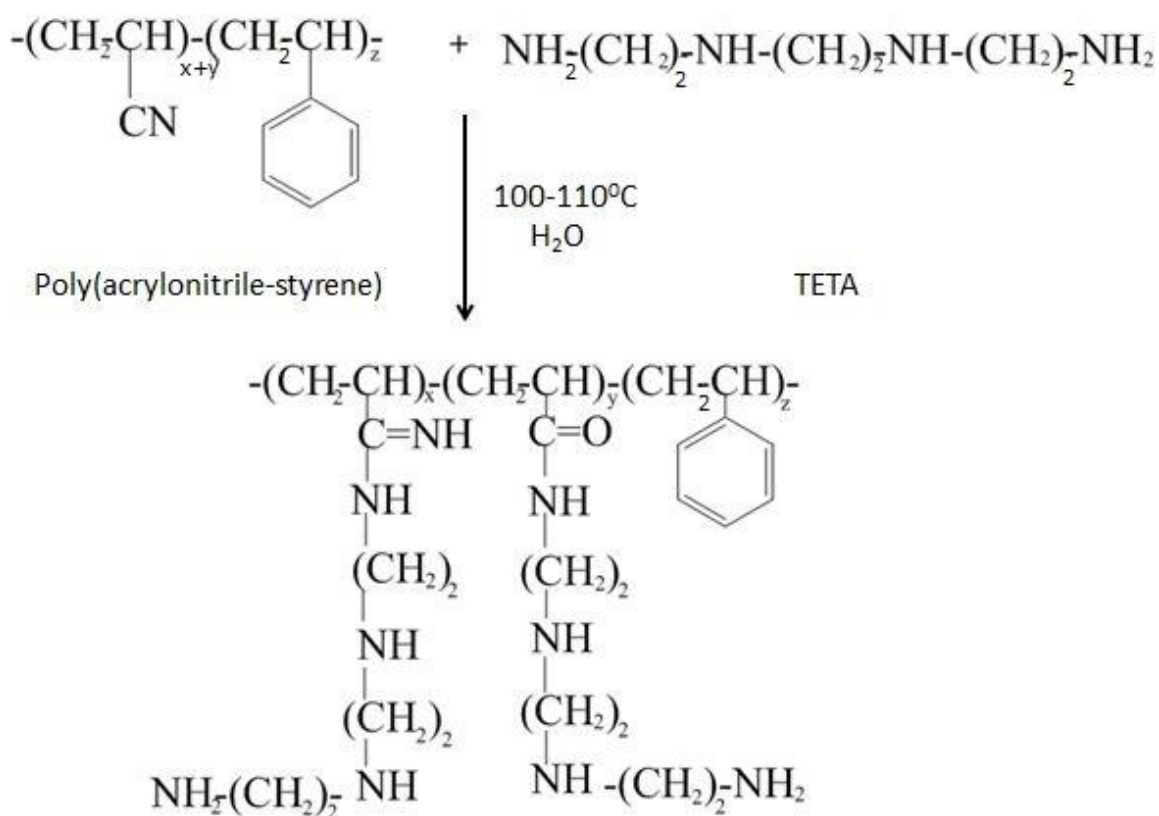
S.No.	Sample	Functionalization composition		
		Resin % (by Wt.)	TETA % (by Wt.)	Water % (by Wt.)
1.	Functionalized polyacrylonitrile resin [F1-PAN]	4.82	46.93	48.23
2.	Functionalized poly(acrylonitrile-styrene) copolymer resin [F1-PANS]	4.82	46.93	48.23
3.	Functionalized poly(acrylonitrile-acrylamide) copolymer resin [F1-PANAm]	4.82	46.93	48.23
4.	Functionalized poly(acrylonitrile-methacrylic acid) copolymer resin [F1-PANMA]	4.82	46.93	48.23
5.	Functionalized polyacrylonitrile resin [F2-PAN]	3.268	47.70	49.027
6.	Functionalized poly(acrylonitrile-styrene) copolymer resin [F2-PANS]	3.268	47.70	49.027
7.	Functionalized poly(acrylonitrile-acrylamide) copolymer resin [F2-PANAm]	3.268	47.70	49.027
8.	Functionalized poly(acrylonitrile-methacrylic acid) copolymer resin [F2-PANMA]	3.268	47.70	49.027

3.2.6 Functionalization method:

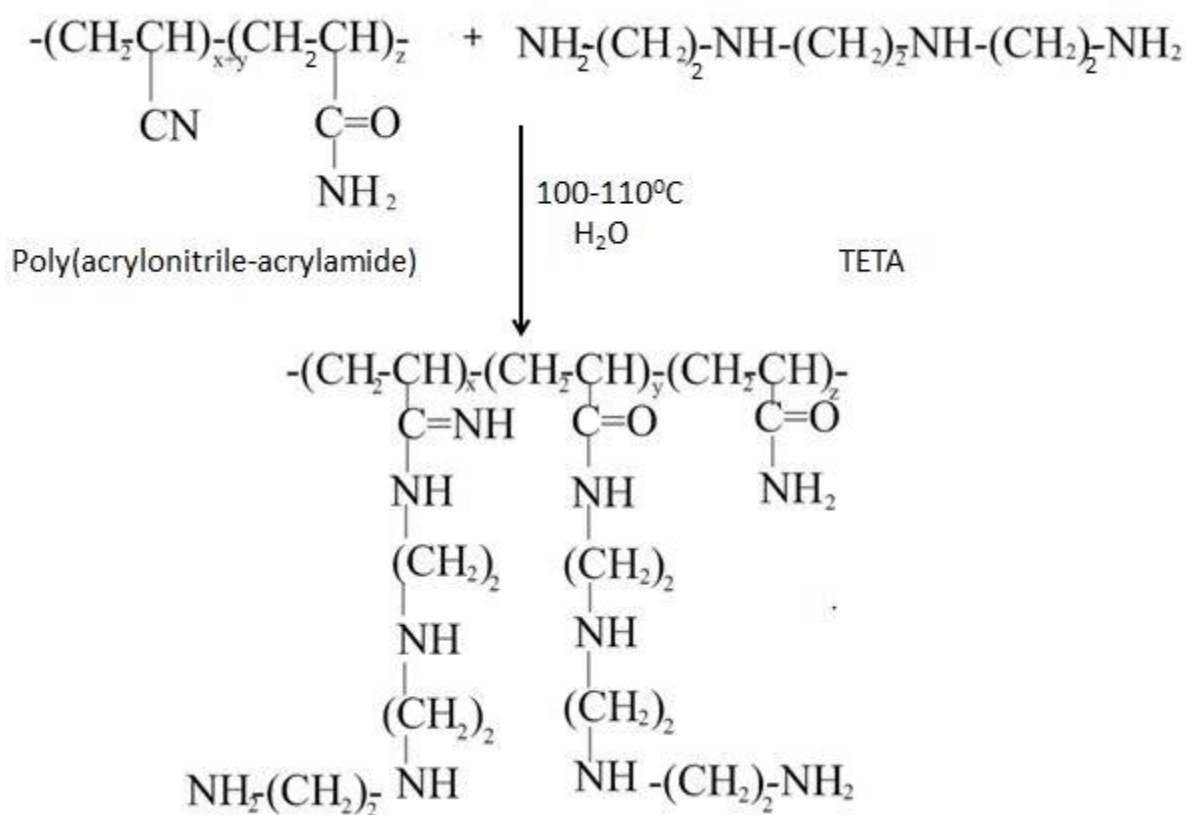
Functionalized PAN based resins were prepared by adding 5 g of resin in 50 mL triethylenetetramine (50 mL of 50 % v/v in water) and 5g of resin in 75 mL triethylenetetramine (75 mL of 75 % v/v in water) in conical flasks. The reaction mixture was stirred for 5 h at 105-115 °C for 5 h. The completion of the reaction was accomplished as the gelation occurs. The resins were separated from the solution by filtration. Resins were then neutralised by its repeated washing in distilled water. Resins were kept in an oven overnight to be dried and stored in desiccator prior to use in sorption studies of heavy metals. The processes of functionalization are shown below (scheme 3.5-3.8).



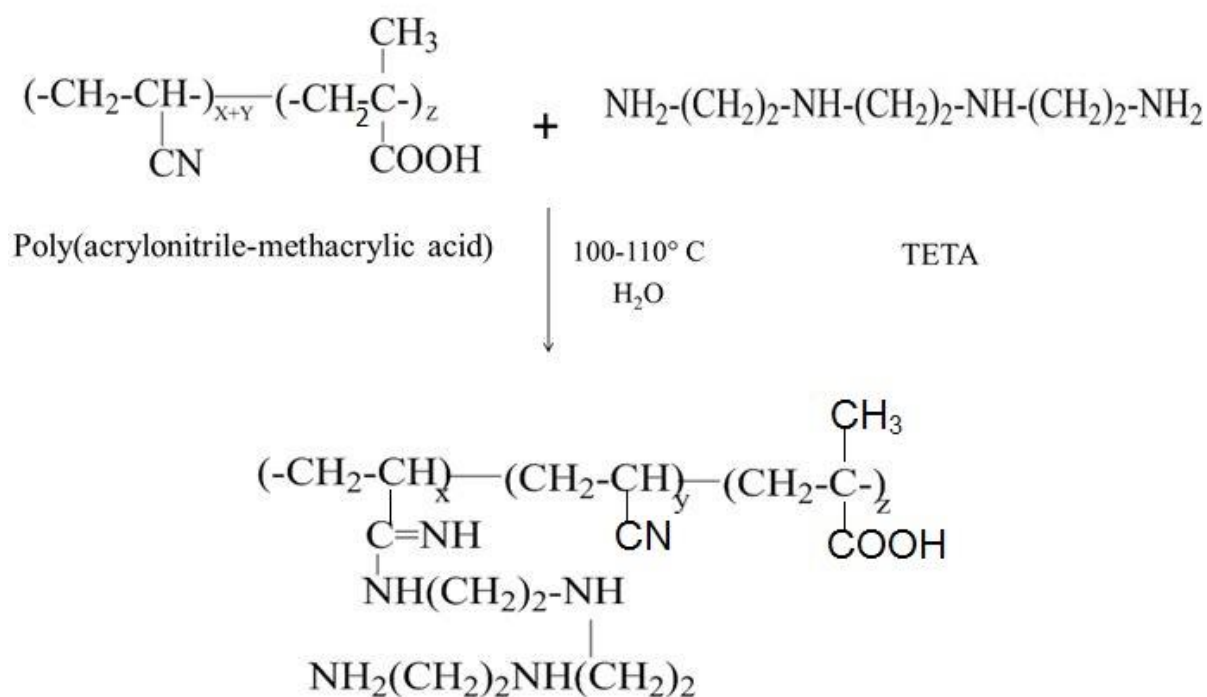
Scheme 3.5: Functionalization reaction of PAN resin



Scheme 3.6: Functionalization reaction of PANS copolymer resin



Scheme 3.7: Functionalization reaction of PANAm copolymer resin



Scheme 3.8: Functionalization reaction of PANMA copolymer resin

3.2.7 Sorption of metal ions:

Sorption process was carried out by adding 0.1 g of resins in solution of iron (Fe^{2+}) and mercury (Hg^{2+}) ions. Solutions containing Fe^{2+} and Hg^{2+} were prepared by adding 0.166 g of ferrous sulphate (FeSO_4) and 0.337 g of $\text{Hg}_2(\text{NO}_3)_2$ (mercurous nitrate) salts in 30 mL of distilled water. Flasks containing solution of salt and resin were stirred for 2 h. After 2 h resins were separated from the solution by filtration and resins were rinsed with distilled water. These metal-resins complexes prepared by the above process were dried in an oven at 50°C .

3.2.8 Molecular weight determination:

The Viscosity average molecular weight was calculated using Ostwald viscometer. 20 solutions of concentrations 0.100, 0.125, 0.150, 0.175 and 0.200 g/dl each of polyacrylonitrile and its copolymers in DMF (Dimethyl formamide) were prepared. First by taking only solvent, i.e., DMF was filled in the U-tube up to the mark above the bulb lower down on the other arm, and then solution was drawn into the upper bulb by suction, and then allowed to flow down through the capillary into the lower bulb. Two marks (one above and one below the upper bulb) indicate

a known volume. The time required for the solution to flow through a capillary of a known diameter of a certain factor between two marked points was measured. Similarly time required for different concentration (0.100, 0.125, 0.150, 0.175 and 0.200 g/dl) solutions were also measured. Required calculations were performed to calculate the viscosity average molecular weight and consequently number average and weight average molecular weight of the polyacrylonitrile and its copolymers.

Determination of viscosity average molecular weight:

The viscosity average molecular weight was determined by using Ostwald Viscometer (fig. 3.1). The viscosity data for PAN and its copolymers is given in tables 3.2-3.5. The plots of η_{sp}/C (reduced viscosity) v/s C (concentration) for PAN and its copolymers in DMF at 30°C are shown below (fig. 3.2-3.5), from which intrinsic viscosity $[\eta]$ is determined by extrapolating the line (η_{sp}/C) to zero concentration. The $[\eta]$ is dependent on polymer, solvent and temperature. So, the experiment was carried out more precisely at constant temperature of 30°C.

The viscosity average molecular weight was determined according to Mark-Houwink equation $[\eta] = KM^a$, where $[\eta]$ is the intrinsic viscosity, M is the molecular weight, a and K are constant for a particular polymer/solvent/temperature system. For Polyacrylonitrile in DMF at 30°C the K and a value are 3.93×10^{-4} and 0.75 respectively (data from polymer Handbook). Finally the viscosity average molecular weight is found.

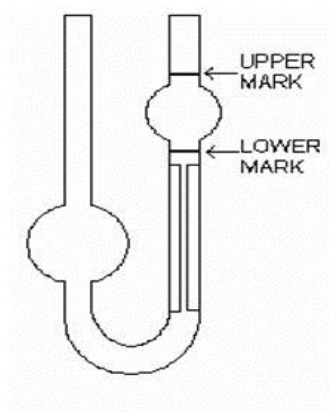


Fig. 3.1: Schematic diagram of Ostwald Viscometer

Table 3.2: Viscosity data for PAN in DMF at 30°C:

Concentration, C, (g/dl)	Flow time (Sec)	Relative viscosity ($t/t_0=\eta_r$)	Specific viscosity ($\eta_{sp} = \eta_r - 1$)	Reduced viscosity ($\eta_{sp}/C = \eta_{red}$) (dl/g)	$\ln \eta_r$	Intrinsic viscosity ($\ln \eta_r/C$) (dl/g)
0.100	1.55	1.29	0.29	2.9	0.255	2.55
0.125	1.66	1.38	0.38	3.04	0.322	2.57
0.150	1.77	1.48	0.48	3.17	0.392	2.60
0.175	1.87	1.57	0.57	3.19	0.443	2.53
0.200	1.96	1.64	0.64	3.21	0.496	2.48

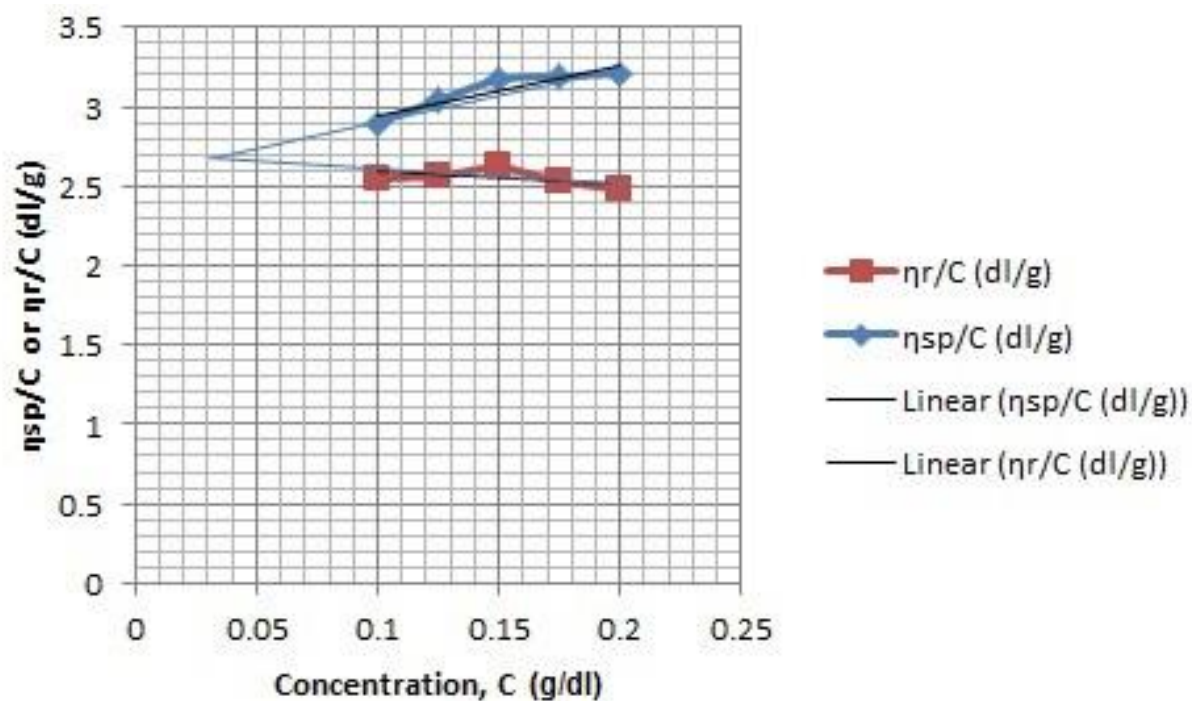


Fig. 3.2: Plot of η_{sp}/C or η_r/C versus C for PAN in DMF at 30°C

Table 3.3: Viscosity data for PANS in DMF at 30°C:

Concentration, C, (g/dl)	Flow time (Sec)	Relative viscosity ($t/t_0=\eta_r$)	Specific viscosity ($\eta_{sp} = \eta_r - 1$)	Reduced viscosity ($\eta_{sp}/C = \eta_{red}$) (dl/g)	$\ln \eta_r$	Intrinsic viscosity ($\ln \eta_r/C$) (dl/g)
0.100	1.58	1.31	0.31	3.10	0.278	2.78
0.125	1.67	1.39	0.39	3.14	0.331	2.65
0.150	1.78	1.48	0.48	3.20	0.392	2.61
0.175	1.89	1.58	0.58	3.29	0.454	2.59
0.200	1.99	1.66	0.66	3.30	0.506	2.53

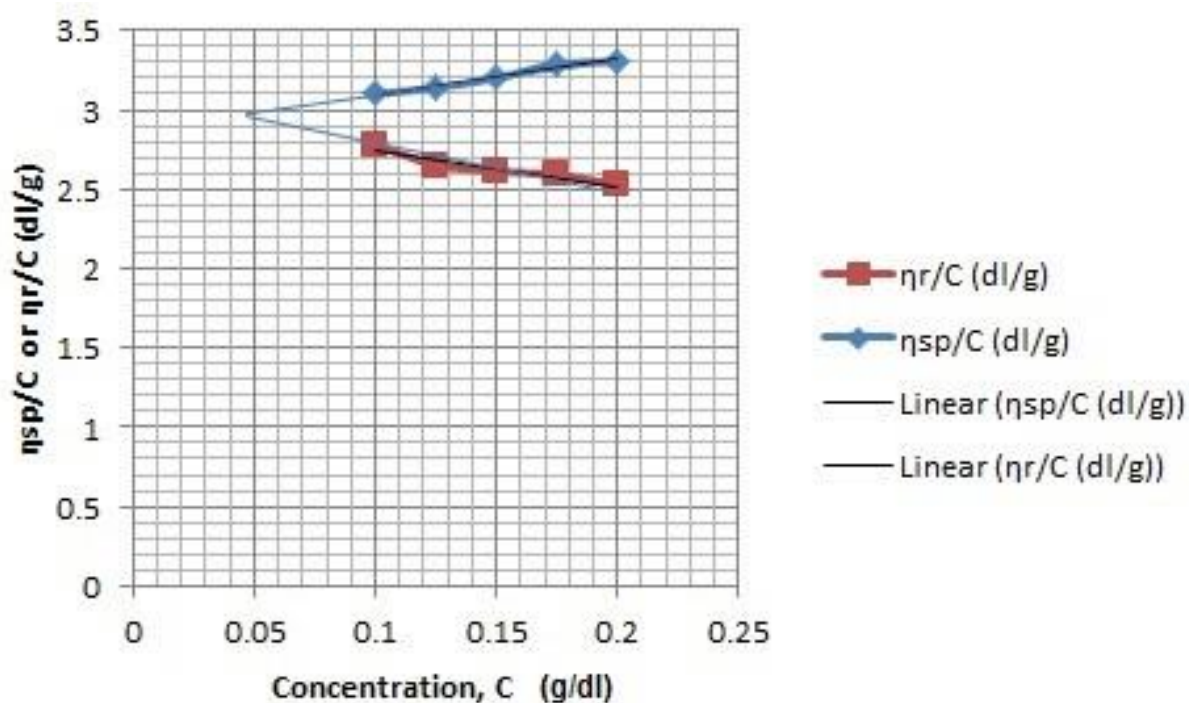


Fig. 3.3: Plot of η_{sp}/C or η_r/C versus C for PANS copolymer in DMF at 30°C

Table 3.4: Viscosity data for PANAm in DMF at 30°C:

Concentration, C, (g/dl)	Flow time (Sec)	Relative viscosity ($t/t_0=\eta_r$)	Specific viscosity ($\eta_{sp} = \eta_r - 1$)	Reduced viscosity ($\eta_{sp}/C = \eta_{red}$) (dl/g)	$\ln \eta_r$	Intrinsic viscosity ($\ln \eta_r/C$) (dl/g)
0.100	1.60	1.33	0.33	3.30	0.285	2.85
0.125	1.71	1.42	0.42	3.44	0.358	2.84
0.150	1.83	1.53	0.53	3.53	0.425	2.83
0.175	1.94	1.63	0.63	3.56	0.489	2.79
0.200	2.07	1.73	0.73	3.65	0.548	2.74

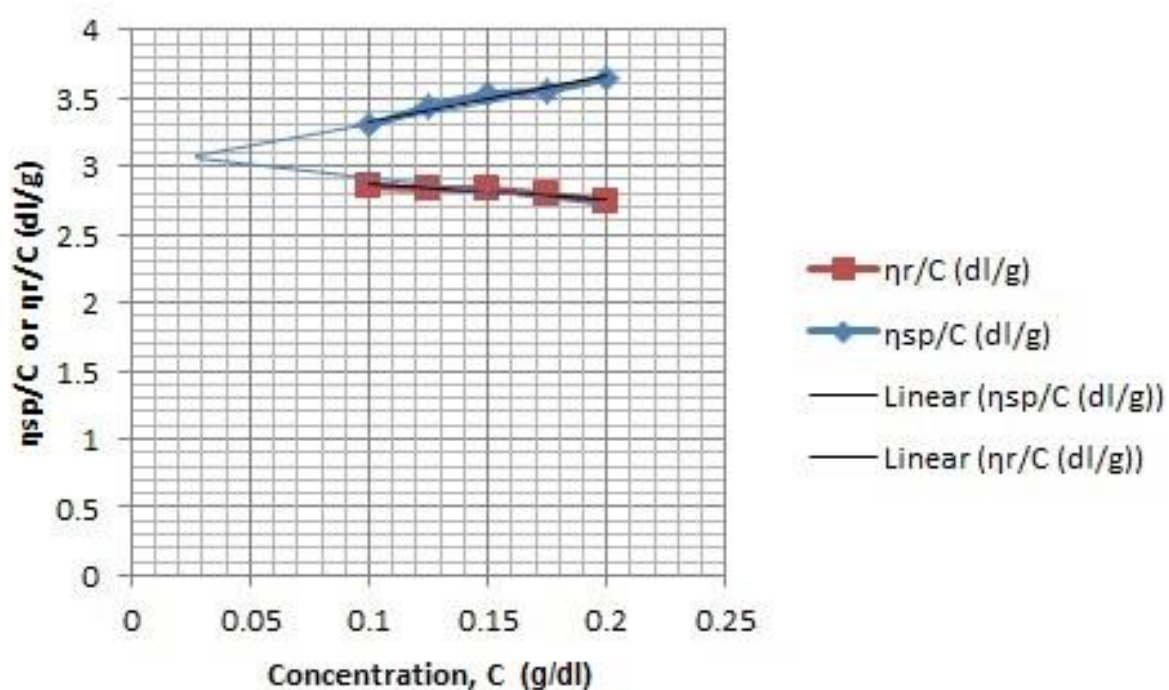


Fig. 3.4: Plot of η_{sp}/C or η_r/C versus C for PANAm copolymer in DMF at 30°C

Table 3.5: Viscosity data for PANMA in DMF at 30°C:

Concentration, C, (g/dl)	Flow time (Sec)	Relative viscosity ($t/t_0=\eta_r$)	Specific viscosity ($\eta_{sp} = \eta_r - 1$)	Reduced viscosity ($\eta_{sp}/C = \eta_{red}$) (dl/g)	$\ln \eta_r$	Intrinsic viscosity ($\ln \eta_r/C$) (dl/g)
0.100	1.63	1.36	0.36	3.6	0.307	3.07
0.125	1.75	1.46	0.46	3.68	0.378	3.02
0.150	1.88	1.57	0.57	3.80	0.451	3.00
0.175	2.02	1.68	0.68	3.89	0.519	2.96
0.200	2.16	1.81	0.81	4.00	0.587	2.90

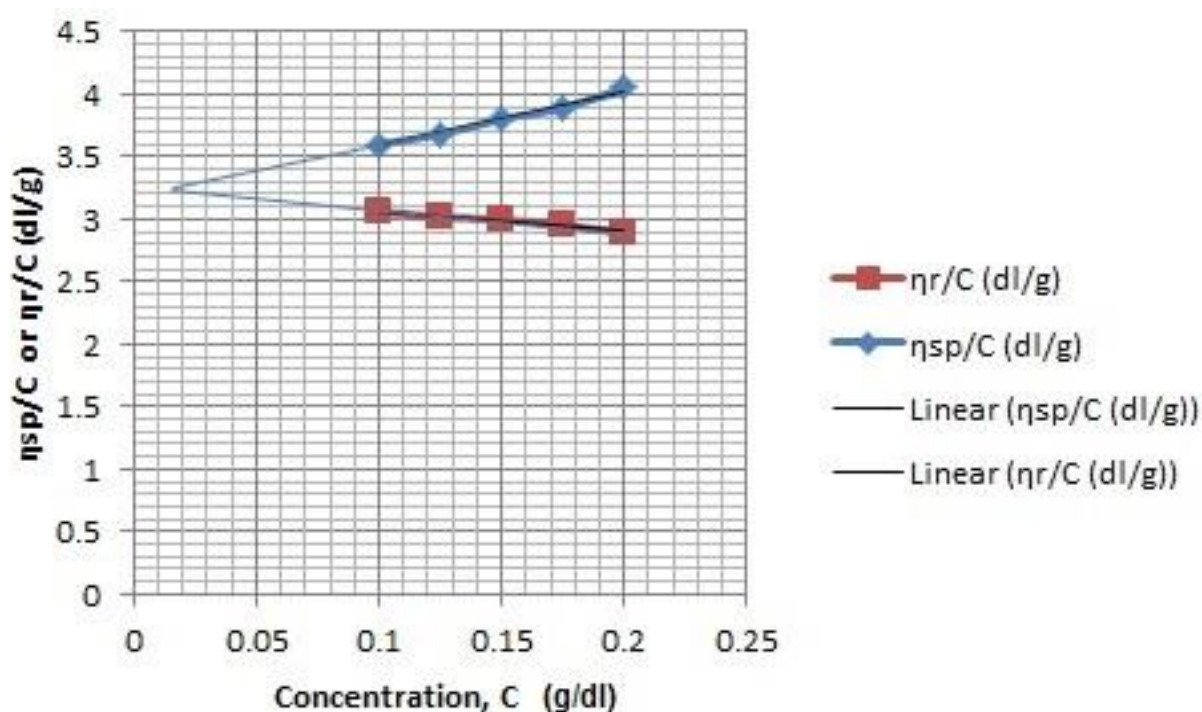


Fig. 3.5: Plot of η_{sp}/C or η_r/C versus C for PANMA copolymer in DMF at 30°C

3.3 CHARACTERIZATION

3.3.1 Fourier Transform Infrared Spectroscopy

To study the functional groups present in the resulting resins/polymer formed FTIR was carried out. Fourier transform infrared spectroscopy is a technique which is used to obtain an infrared spectrum of absorption, emission, photoconductivity or Raman scattering of a solid, liquid or gas.

Infrared (IR) spectroscopy is one of the most common spectroscopic techniques used by organic and inorganic chemists. Simply, it is the absorption measurement of different IR frequencies by a sample positioned in the path of an IR beam. The main goal of IR spectroscopic analysis is to determine the chemical functional groups in the sample. Infrared spectroscopy has been a workhorse technique for materials analysis in the laboratory for over seventy years. An infrared spectrum represents a fingerprint of a sample with absorption peaks which correspond to the frequencies of vibrations between the bonds of the atoms making up the material. Because each different material is a unique combination of atoms, no two compounds produce the exact same infrared spectrum. Therefore, infrared spectroscopy can result in a positive identification (qualitative analysis) of every different kind of material. In addition, the size of the peaks in the spectrum is a direct indication of the amount of material present. With modern software algorithms, infrared is an excellent tool for quantitative analysis. Different functional groups absorb characteristic frequencies of IR radiation. Using various sampling accessories, IR spectrometers can accept a wide range of sample types such as gases, liquids and solids.

Equipment Specifications:

Thermo Scientific Nicolet 380 Spectrometer (fig. 3.6)

Spectral range: $7800 - 350 \text{ cm}^{-1}$ using proprietary KBr beam splitter.

Optical resolution $< 0.9 \text{ cm}^{-1}$ resolution (standard)

Wavenumber precision- Better than 0.01 cm^{-1} precision at 2000 cm^{-1}



Fig. 3.6: Nicolet 380 Fourier Transform Infrared Spectrometer

3.3.2 Energy-Dispersive X-ray Spectroscopy

EDS makes use of the X-ray spectrum emitted by a solid sample bombarded with a focused beam of electrons to obtain a localized chemical analysis. All elements from atomic number 4 (Be) to 92 (U) can be detected in principle, though not all instruments are equipped for 'light' elements ($Z < 10$). Qualitative analysis involves the identification of the lines in the spectrum and is fairly straightforward owing to the simplicity of X-ray spectra. Quantitative analysis (determination of the concentrations of the elements present) entails measuring line intensities for each element in the sample and for the same elements in calibration Standards of known composition.

By scanning the beam in a television-like raster and displaying the intensity of a selected X-ray line, element distribution images or 'maps' can be produced. Also, images produced by electrons collected from the sample reveal surface topography or mean atomic number differences according to the mode selected. The scanning electron microscope, which is closely related to the electron probe, is designed primarily for producing electron images, but can also be used for element mapping, and even point analysis, if x-ray spectrometer is added. EDS was done by Hitachi Hi Technologies Scanning Electron Microscope S-3700 N.

Equipment specifications:

Hitachi Hi Technologies Scanning Electron Microscope S-3700 N (fig. 3.7)

Specimen size: 1x1 cm

Operating voltage: 2.5kv 15 KV

Resolution: 3.0 nm at 30 KV (High vacuum mode)



Fig. 3.7: Hitachi Hi Technologies S_3700 N Scanning Electron Microscope

3.4 ANALYSIS**3.4.1 Scanning Electron Microscopy**

SEM was carried out to study the morphology of the resins/polymers produced. A scanning electron microscope is a type of electron microscope that produces images of a sample by scanning it with a focused beam of electrons. The electrons interact with electrons in the sample, producing various signals that can be detected and that contain information about the sample's

surface topography and composition. The electron beam is generally scanned in a raster scan pattern, and the beam's position is combined with the detected signal to produce an image. SEM can achieve resolution better than 1 nm (nanometer). Specimens can be observed in high vacuum, in low vacuum, and (in environmental SEM) in wet conditions.

The most common mode of detection is by secondary electrons emitted by atoms excited by the electron beam. The number of secondary electrons is a function of the angle between the surface and the beam. On a flat surface, the plume of secondary electrons is mostly contained by the sample, but on a tilted surface, the plume is partially exposed and more electrons are emitted. By scanning the sample and detecting the secondary electrons, an image displaying the tilt of the surface is created.

The equipment used was Hitachi-S-3700N (fig. 3.7)

3.4.2 Thermogravimetric Analysis

Thermogravimetric analysis or thermal gravimetric analysis is a method of thermal analysis in which changes in physical and chemical properties of materials are measured as a function of increasing temperature (with constant heating rate), or as a function of time (with constant temperature and/or constant mass loss).

TGA can provide information about physical phenomena, such as second-order phase transitions, including vaporization, sublimation, adsorption, adsorption, and desorption. Likewise, TGA can provide information about chemical phenomena including chemisorptions, desolvation (especially dehydration), decomposition, and solid-gas reactions (e.g., oxidation or reduction). TGA is commonly used to determine selected characteristics of materials that exhibit either mass loss or gain due to decomposition, oxidation, or loss of volatiles (such as moisture). Common applications of TGA are (1) materials characterization through analysis of characteristic decomposition patterns, (2) studies of degradation mechanisms and reaction kinetics, (3) determination of organic content in a sample, and (4) determination of inorganic (e.g. ash) content in a sample, which may be useful for corroborating predicted material structures or simply used as a chemical analysis. Thermogravimetric analysis relies on a high degree of precision in three measurements: mass change, temperature, and temperature change. Therefore, the basic instrumental requirements for TGA are a precision balance with a pan loaded with the sample, and a programmable furnace. The furnace can be programmed either for a constant heating rate, or for heating to acquire a constant mass loss with time. Though a constant heating rate is more common, a constant mass loss rate can illuminate specific reaction

kinetics. Regardless of the furnace programming, the sample is placed in a small, electrically heated furnace equipped with a thermocouple to monitor accurate measurements of the temperature by comparing its voltage output with that of the voltage-versus-temperature table stored in the computer's memory. A reference sample may be placed on another balance in a separate chamber. The atmosphere in the sample chamber may be purged with an inert gas to prevent oxidation or other undesired reactions.

Equipment specifications:

TA Instruments Thermogravimetric Analyzer Q50 [fig.3.8]

Maximum Sample Weight 1 g

Temperature Range Ambient to 1000°C

Controlled Heating Rate 0.1 to 100°C/min

Isothermal Temp Accuracy $\pm 1^{\circ}\text{C}$



Fig. 3.8: TA Instruments Thermogravimetric Analyzer Q 50

3.4.3 Differential Scanning Colorimeter:

A differential scanning calorimeter measures the heat of sample relative to a reference and heats the sample with a linear temperature ramp. Endothermic heat flows into the sample. Exothermic heat flows out of the sample. Differential Scanning Colorimetry, measures the heat flows and temperatures associated with transitions in materials as a function of time and temperature in a controlled atmosphere. These measurements provide quantitative and qualitative information about physical and chemical changes that involve endothermic or exothermic processes or changes in heat capacity. Differential scanning colorimetry monitors heat effects associated with phase transitions and chemical reactions as a function of temperature. In a DSC the difference in heat flow to the sample and a reference at the same temperature, is recorded as a function of temperature. The reference is an inert material such as alumina, or just an empty aluminium pan. The temperature of both the sample and reference are increased at a constant rate.

Equipment specifications:

TA Instruments DSC Q20 (fig. 3.9)

Temperature Range: Ambient to 725 °C

Temperature Accuracy: ± 0.1 °C

Sensitivity: 1.0 Mw



Fig. 3.9: TA Instruments DSC Q20

3.4.4 Dynamic Mechanical Analysis

Dynamic mechanical analysis (abbreviated DMA, also known as dynamic mechanical spectroscopy) is a technique used to study and characterize materials. It is most useful for studying the viscoelastic behaviour of polymers. A sinusoidal stress is applied and the strain in the material is measured, allowing one to determine the complex modulus. The temperature of the sample or the frequency of the stress are often varied, leading to variations in the complex modulus; this approach can be used to locate the glass transition temperature of the material, as well as to identify transitions corresponding to other molecular motions. One important application of DMA is measurement of the glass transition temperature of polymers. Amorphous polymers have different glass transition temperatures, above which the material will have rubbery properties instead of glassy behaviour and the stiffness of the material will drop dramatically with an increase in viscosity. At the glass transition, the storage modulus decreases dramatically and the loss modulus reaches a maximum. Temperature-sweeping DMA is often used to characterize the glass transition temperature of a material. The viscoelastic property of a polymer is studied by dynamic mechanical analysis where a sinusoidal force (stress σ) is applied to a material and the resulting displacement (strain) is measured. For a perfectly elastic solid, the resulting strain and the stress will be perfectly in phase. For a purely viscous fluid, there will be a 90° phase lag of strain with respect to stress. Viscoelastic polymers have the characteristics in between where some phase lag will occur during DMA tests.

The instrumentation of a DMA consists of a displacement sensor such as a linear variable differential transformer, which measures a change in voltage as a result of the instrument probe moving through a magnetic core, a temperature control system or furnace, a drive motor (a linear motor for probe loading which provides load for the applied force), a drive shaft support and guidance system to act as a guide for the force from the motor to the sample, and sample clamps in order to hold the sample being tested. Depending on what is being measured, samples will be prepared and handled differently.

Equipment specifications:

Perkin Elmer Dynamic Mechanical Analyser 8000 (fig. 3.10)

Temperature Range:

Standard furnace: -190 °C to 400 °C

High temperature: furnace: -190 °C to 600 °C

Immersion bath: -196 °C to 150 °C

Stiffness Range: 2×10^2 to 1×10^8 N/m resolutions 2 N/m



Fig. 3.10: Perkin Elmer Dynamic Mechanical Analyser 8000

CHAPTER-4

RESULTS AND DISCUSSION

4.1 Molecular weight determination:

An average molecular weight of the PAN and its copolymer resins was determined and the measurement details have been presented in the previous chapter. The data of average molecular weight and viscosity data of the samples are given in the following table 4.1.

Table 4.1: Molecular weight and viscosity measurement data of the samples

S.No.	Sample	η (Viscosity) (dl/g)	Molecular weight
1.	PAN resin	2.70	1,30,606
2.	PANS resin	3.00	1,50,304
3.	PANAm resin	3.10	1,57,022
4.	PANMA resin	3.25	1,67,233

The data presented in the above table show that the PAN based copolymer resins have higher molecular weight than the PAN resin. PANMA copolymer resin possesses highest molecular weight in comparison to other PAN and its copolymer resins. Also, the viscosity data show that on increasing the viscosity, molecular weight of the resins also increases.

4.2 FTIR Analysis

The FTIR was used to characterize the prepared samples and it confirmed the presence of functional groups in the PAN and its copolymer resins with styrene, acrylamide and methacrylic acid comonomers. In the FTIR spectra of PAN (fig. 4.1), the peak at 2243 cm^{-1} is due to -CN stretch and confirmed the presence of -CN group of acrylonitrile. The peaks at 2939 and 1455 cm^{-1} are assigned to C-H stretch and C-H bending of CH_2 groups.

In the FTIR spectra (fig. 4.2) of PANS copolymer, the peak at 3061 cm^{-1} is due to C-H stretch of the unsaturated carbon. Also the peak at 760 cm^{-1} is due to the presence of phenyl ring of the styrene. The peak at 2238 cm^{-1} is attributed due to -CN group of the acrylonitrile. These characteristic peaks confirmed the presence of acrylonitrile and styrene in the copolymer.

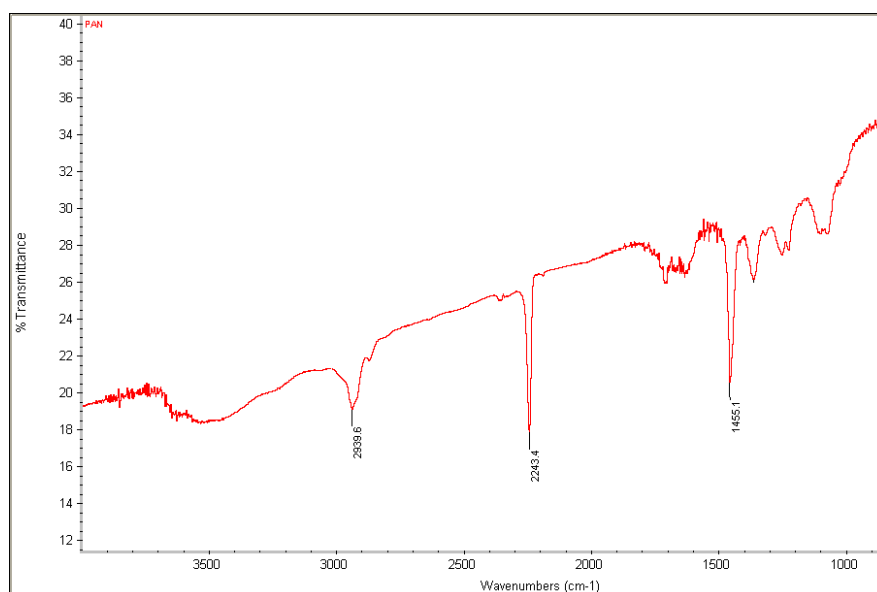


Fig. 4.1: FTIR spectra of PAN resin

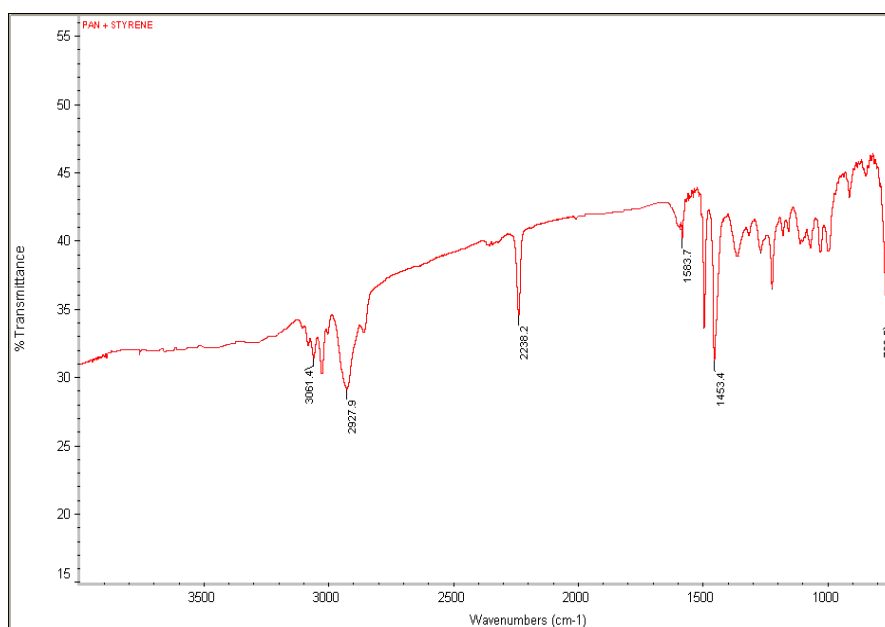


Fig. 4.2: FTIR spectra of PANS copolymer resin

Fig. 4.3 shows the FTIR spectra of PANAm copolymer, the broad peak at 3446 cm^{-1} is attributed due to N-H stretch and the peak at 1681 cm^{-1} is due to C=O stretch. The characteristic peak at 1111 cm^{-1} is due to C-N stretch. All these peaks establish the presence of CONH₂ group in the copolymer. However, other peaks are in the same region as found in case of the PAN homopolymer FTIR spectra.

The FTIR spectra (fig. 4.4) of PANMA copolymer shows the characteristic peak at 3445 cm^{-1} which is attributed due to O-H stretch and the peak at 1735 cm^{-1} is due to C=O stretch. So, these peaks confirmed the presence of -COOH group of the methacrylic acid.

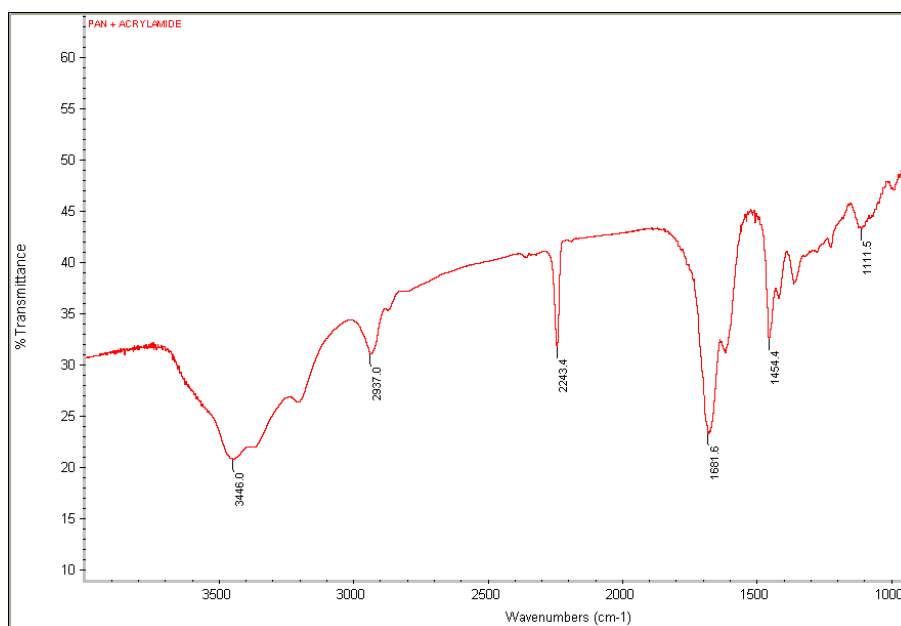


Fig. 4.3: FTIR spectra of PANAm copolymer resin

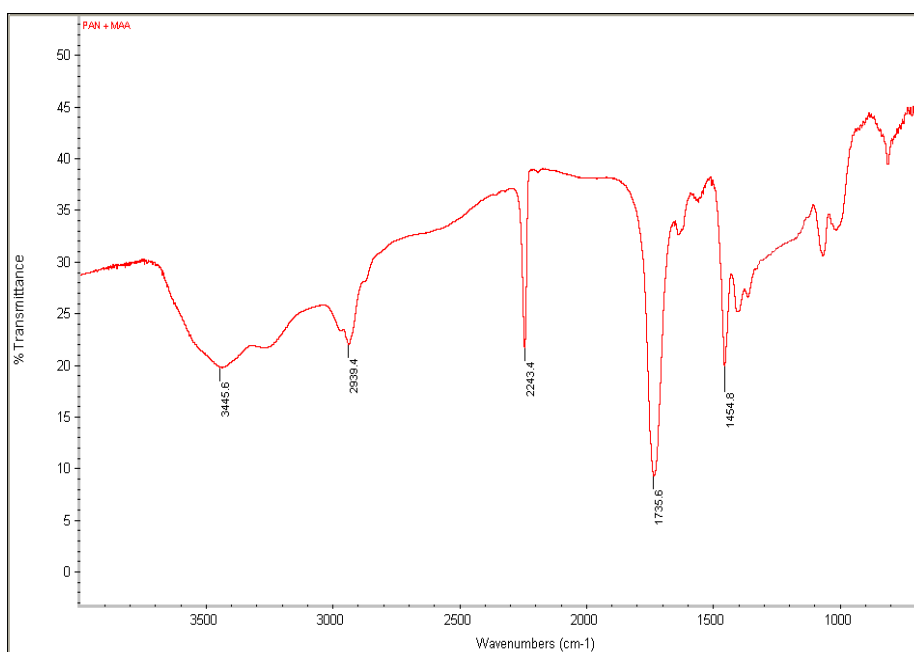


Fig. 4.4: FTIR spectra of PANMA copolymer resin

The FTIR spectra of F1 and F2; PAN, PANS, PANAm and PANMA are shown below in fig. 4.5-4.8. In the FTIR spectra of F1 and F2; PAN, PANS, PANAm and PANMA, the

characteristic peaks at 3414, 3418, 3446 and 3240 cm^{-1} are due to N-H stretch, respectively. The peaks in the region 1640 – 1740 cm^{-1} are due to the C=O stretch and in the region 1550-1650 cm^{-1} are due to the C=N stretch. Also, there are peaks in the region 1020-1120 cm^{-1} due to C-N stretch. The existence of these peaks confirmed the successful functionalization of PAN and its copolymers.

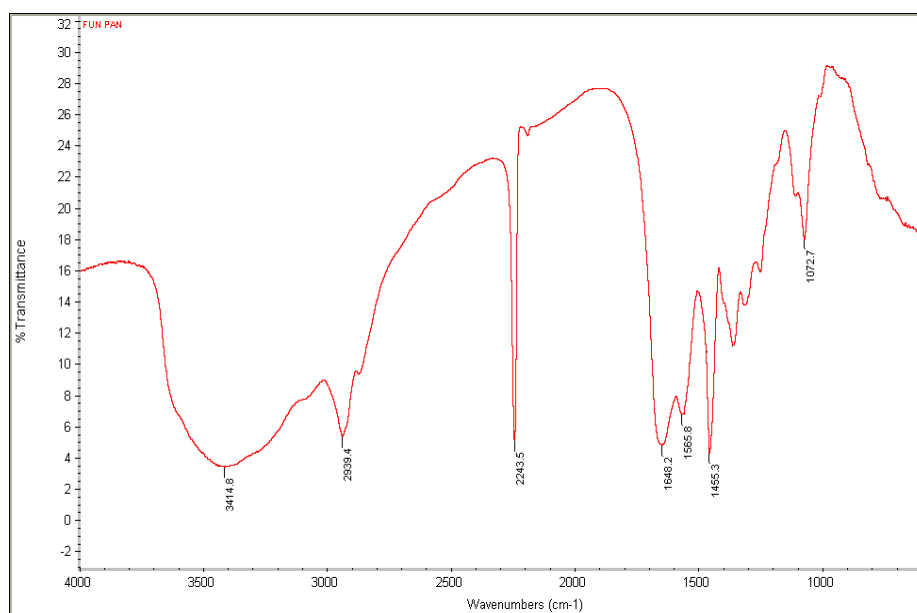


Fig. 4.5: FTIR spectra of functionalized PAN resin

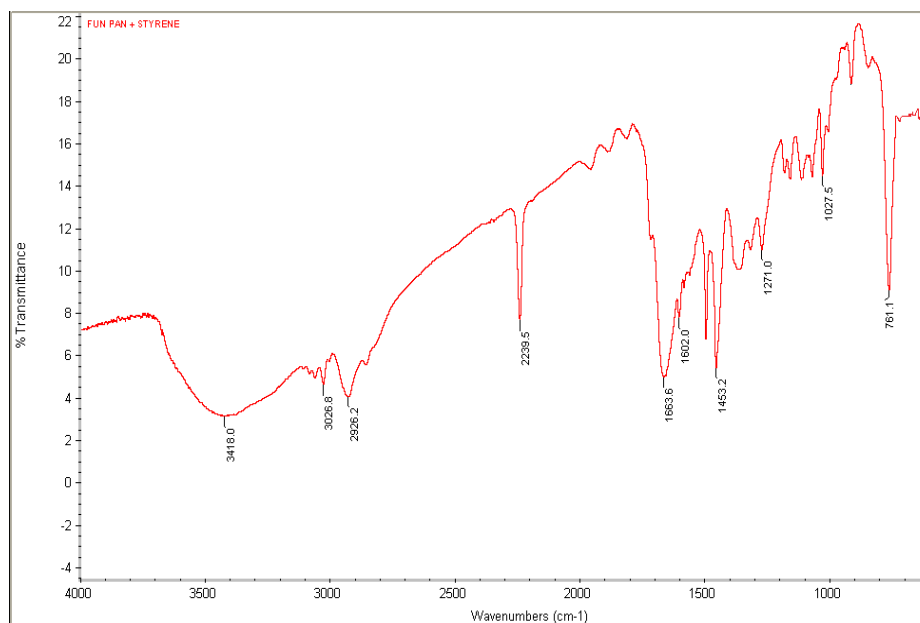


Fig. 4.6: FTIR spectra of functionalized PANS

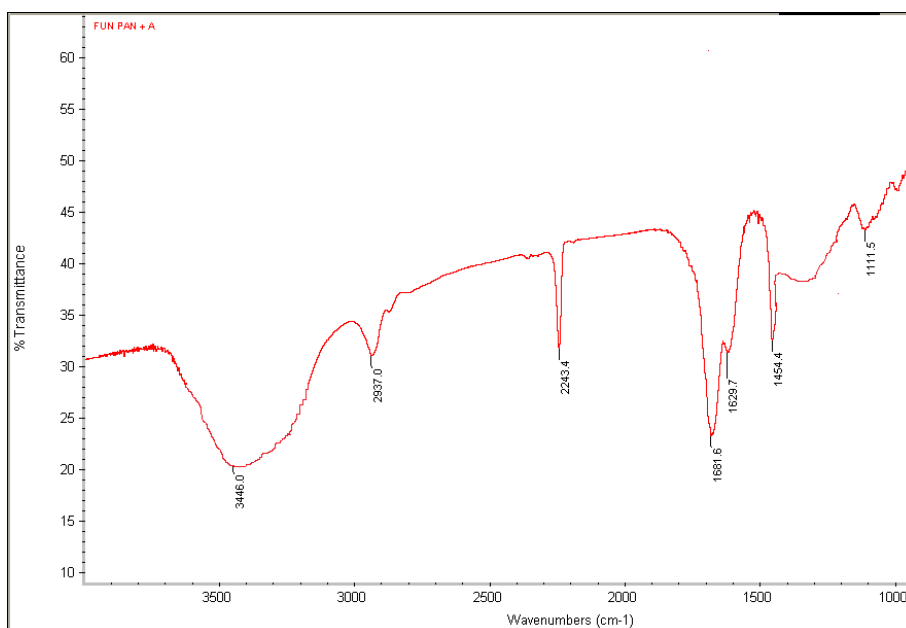


Fig. 4.7: FTIR spectra of functionalized PANAm resin

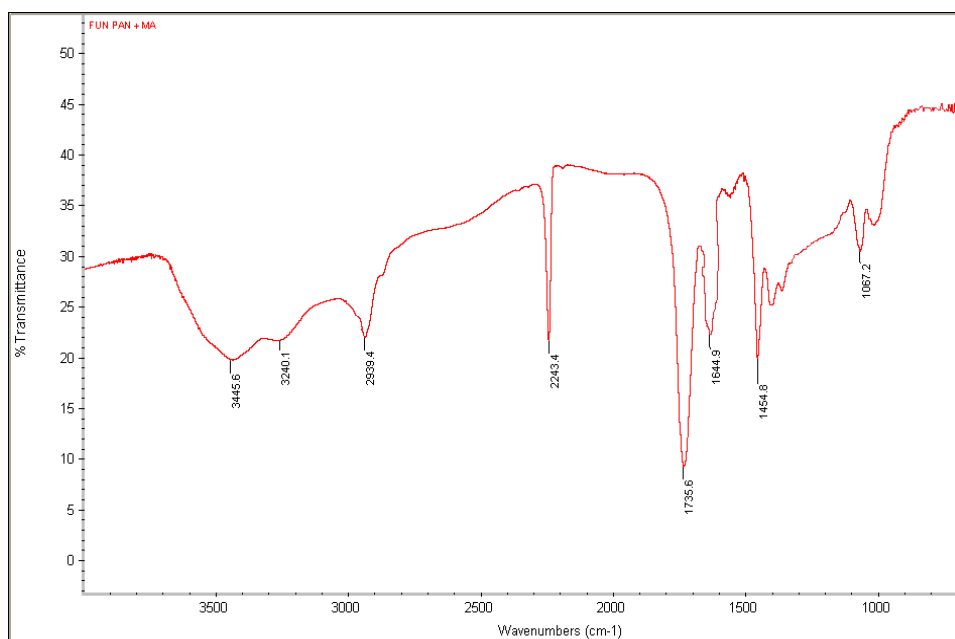


Fig. 4.8: FTIR spectra of functionalized PANMA resin

Thus, we can conclude that the presence of the functional groups such as -CO , -CN , -OH , -NH_2 , -COOH , -CONH_2 etc. have been established in the FTIR spectra. It clearly indicates the formation of functionalized resins.

4.3. EDS Analysis:

In the present study, EDS was used to confirm the adsorption of the metals by the functionalized PAN and its copolymers. The EDS was carried out to detect the presence of Hg^{2+} and Fe^{2+} absorbed by functionalized polymers from their aqueous solution. The EDS graphs F1-PAN, F1-PANS, F1-PANAm, F1-PANMA, F2-PAN, F2-PANS, F2-PANAm and F2-PANMA are shown below (fig. 4.9-4.24).

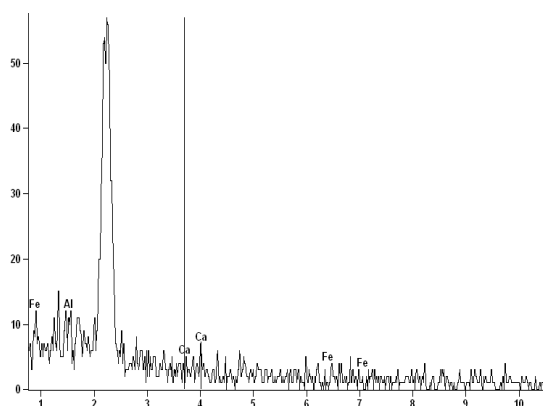


Fig. 4.9: EDS graph of F1-PAN for the adsorption of Fe^{2+}

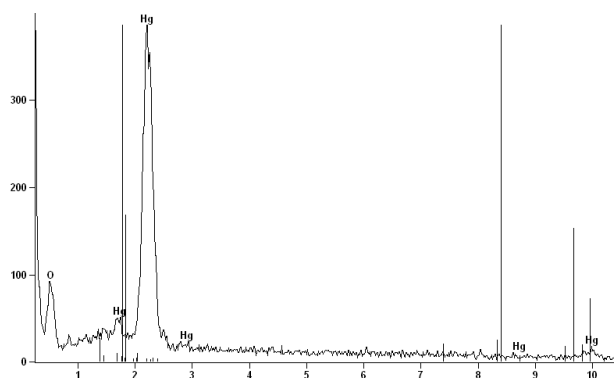


Fig.4.10: EDS graph of F1-PAN for the adsorption of Hg^{2+}

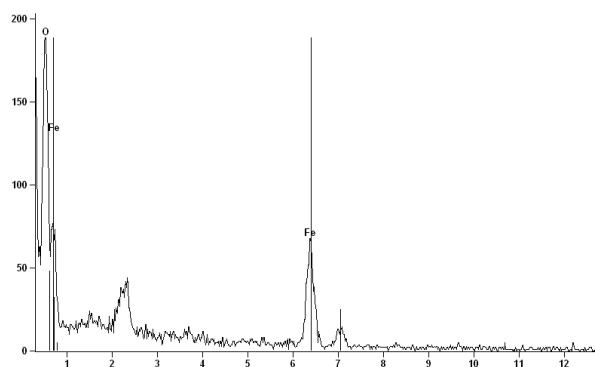


Fig.4.11: EDS graph of F1-PANS for the adsorption of Fe^{2+}

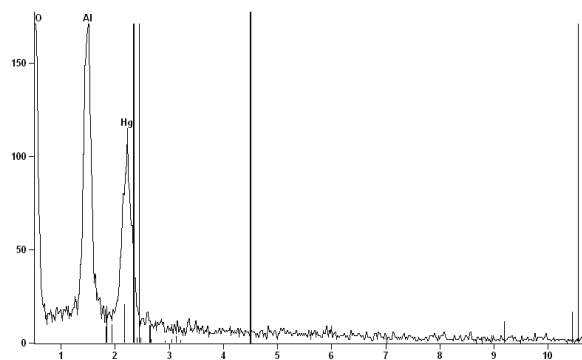


Fig.4.12: EDS graph of F1-PANS for the adsorption of Hg^{2+}

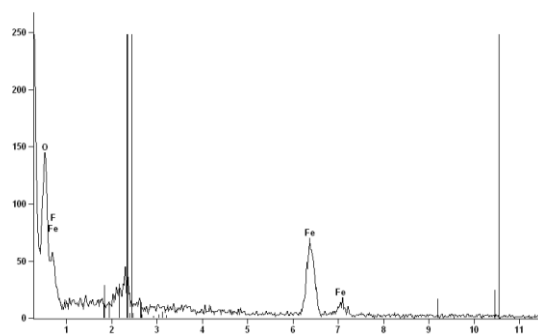


Fig.4.13: EDS graph of F1-PANAm for the adsorption of Fe^{2+}

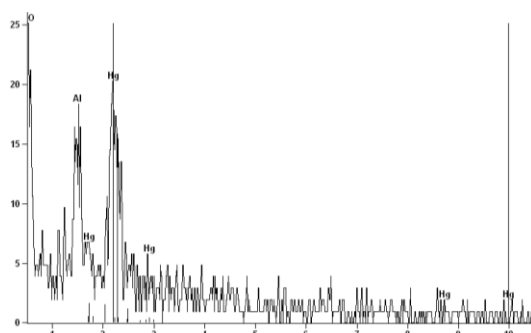


Fig.4.14: EDS graph of F1-PANAm for the adsorption of Hg^{2+}

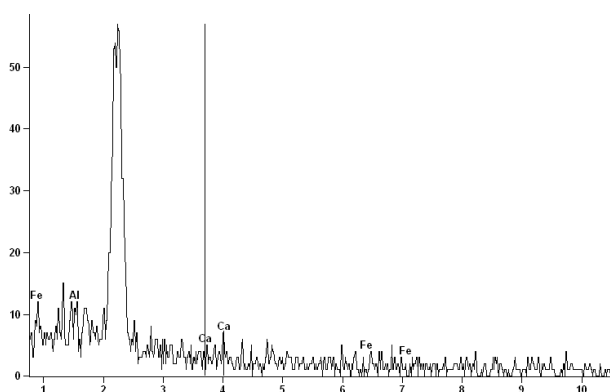


Fig.4.15: EDS graph of F1-PANMA for the adsorption of Fe^{2+}

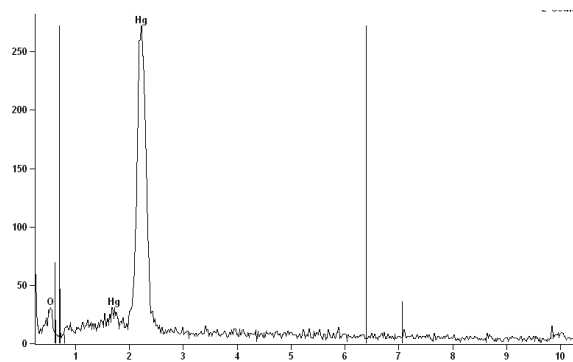


Fig.4.16: EDS graph of F1-PANMA for the adsorption of Hg^{2+}

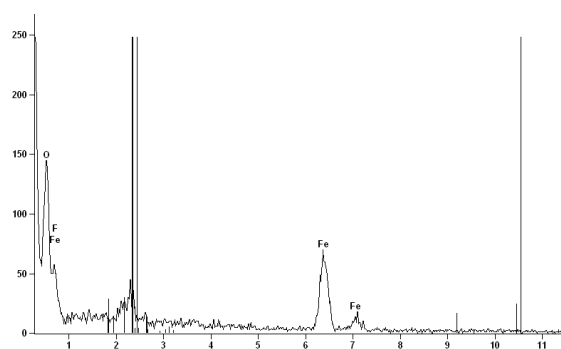


Fig.4.17: EDS graph of F2-PAN for the adsorption of Fe^{2+}

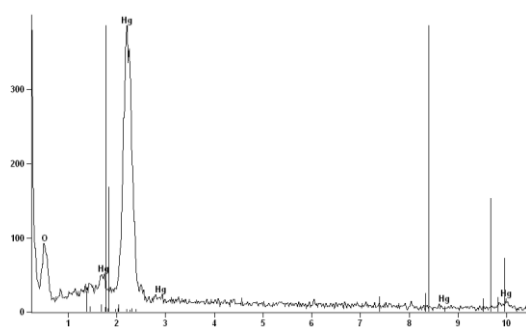


Fig.4.18: EDS graph of F2-PAN for the adsorption of Hg^{2+}

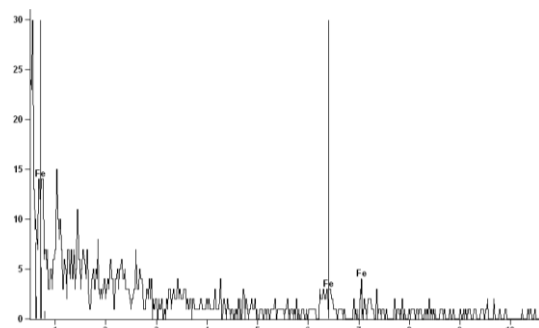


Fig. 4.19: EDS graph of F2-PANS for the adsorption of Fe^{2+}

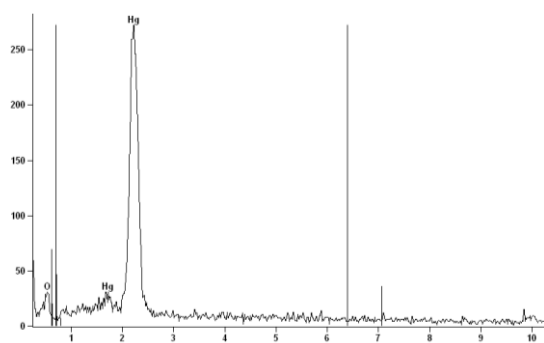


Fig. 4.20: EDS graph of F2-PANS for the adsorption of Hg^{2+}

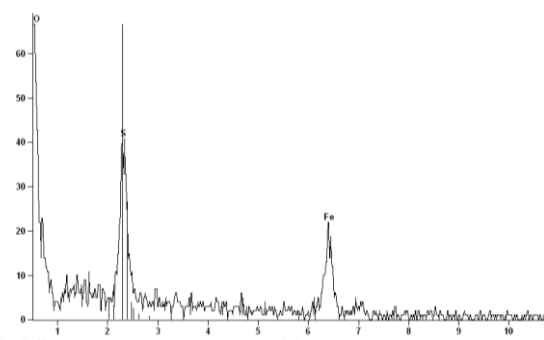


Fig. 4.21: EDS graph of F2-PANAm for the adsorption of Fe^{2+}

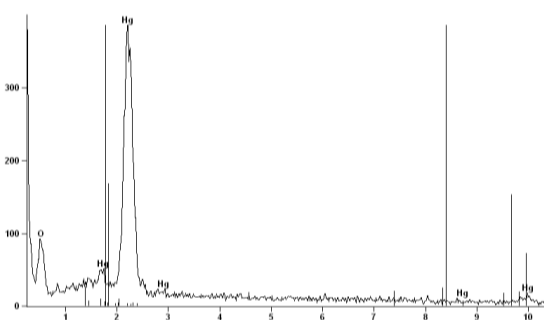


Fig. 4.22: EDS graph of F2-PANAm for the adsorption of Hg^{2+}

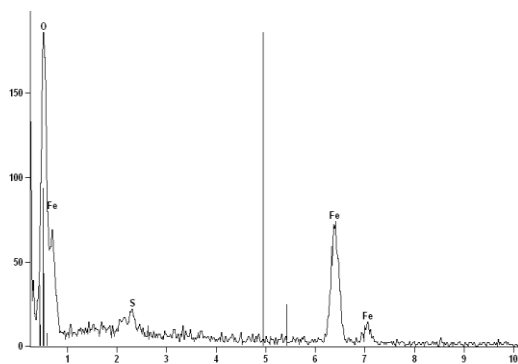


Fig. 4.23: EDS graph of F2-PANMA for the adsorption of Fe^{2+}

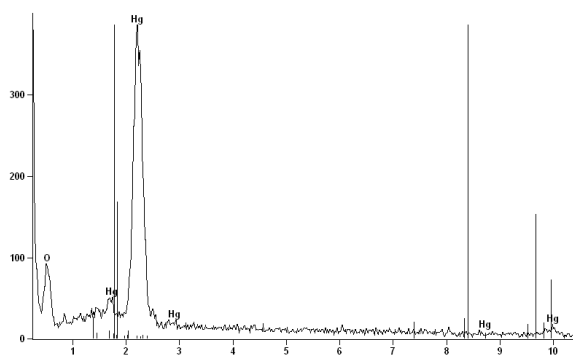


Fig. 4.24: EDS graph of F2-PANMA for the adsorption of Hg^{2+}

For the adsorption of the Hg^{2+} ions from its aqueous solution, F2-PANS shows the best adsorption capacity. The weight percentage obtained for Hg^{2+} in F2-PANS is 86.39 %. For the adsorption of the Fe^{2+} from its aqueous solution, F2-PANMA shows the best adsorption capacity. In this case, the weight percentage obtained for Fe^{2+} ion in F2-PANMA is 87.47 %.

The data given below in table 4.2, represent the wt. % adsorption of Hg^{2+} and Fe^{2+} for various polymer and copolymer resins.

Table 4.2: Wt. % adsorption for Hg^{2+} and Fe^{2+} in various polymer resins

S.No	Sample	Wt % Hg	Wt % Fe
1.	F1-PAN	35.31	45.50
2.	F1-PANS	50.82	50.04
3.	F1-PANAm	57.36	57.59
4.	F1-PANMA	59.00	60.33
5.	F2-PAN	60.45	58.23
6.	F2-PANS	86.39	60.47
7.	F2-PANAm	71.54	59.09
8.	F2-PANMA	74.89	87.47

The graphical representation (fig. 4.25) for the adsorption of heavy metal/metal ions are also given which shows the maximum adsorption by F2-PANS for Hg^{2+} ions and F2-PANMA for Fe^{2+} ions. The EDS results show that the copolymer resins functionalized with higher amount of TETA possess better adsorption capacity. Functionalized copolymer resins of PAN with styrene and methacrylic acid are found to possess higher adsorption capacity for Hg^{2+} and Fe^{2+} , respectively.

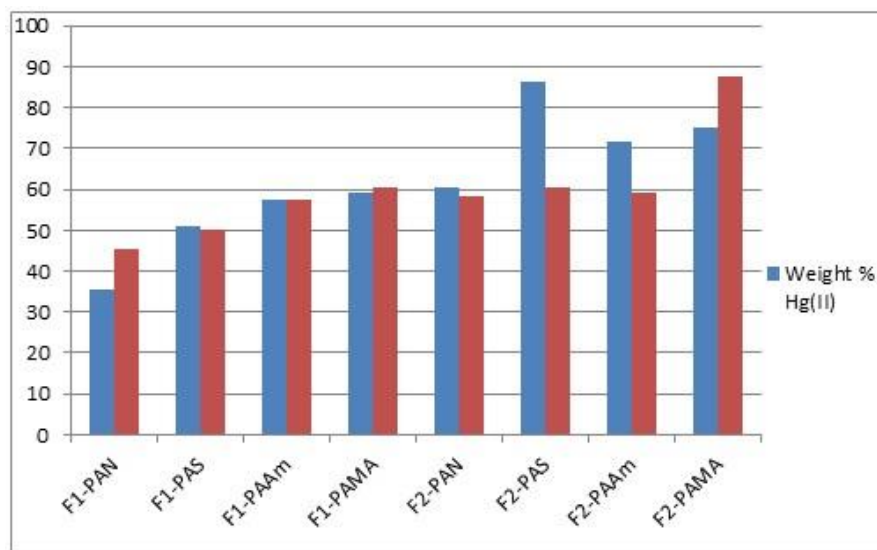


Fig. 4.25: Graphical representation of wt % of Hg^{2+} and Fe^{2+} adsorbed by functionalized resins

4.4 SEM Analysis:

SEM was used to study the surface morphology of the functionalized polymer resins. The SEM micrographs show that the surfaces of the polymer resins are globular. As we know that the presence of pores is necessary for an adsorbent to be more effective. In the present findings, the pores are visible in the SEM micrographs of the polymer resins of varying sizes. SEM micrograph of F2-PANS shows a large number of pores as compared to other polymer resins. This larger number of pores is responsible for the higher adsorption capacity of F2-PANS for Mercury ions as revealed by EDS. Similarly, the polymer resin F2-PANMA with higher adsorption capacity for Iron ion is more porous in nature than other polymer resins. The SEM micrographs of functionalized PAN and its copolymer resins are given below (fig. 4.26-4.33).

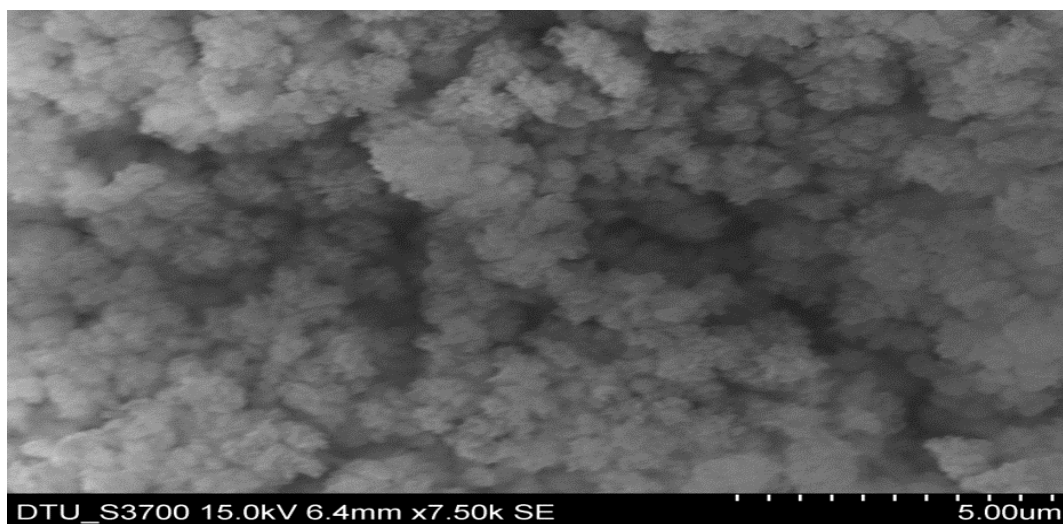


Fig. 4.26: SEM micrograph of F1-PAN

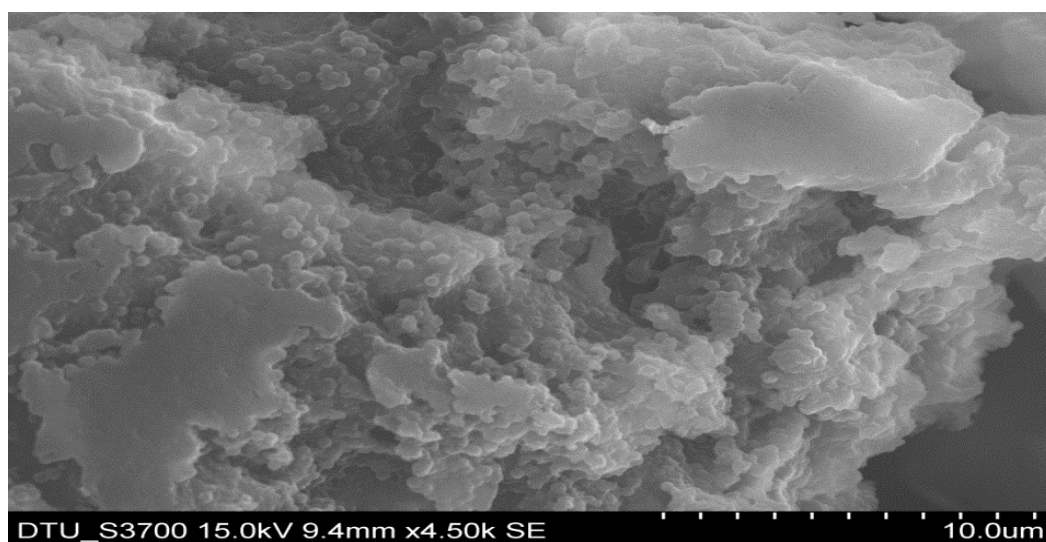


Fig. 4.27: SEM micrograph of F1-PANS

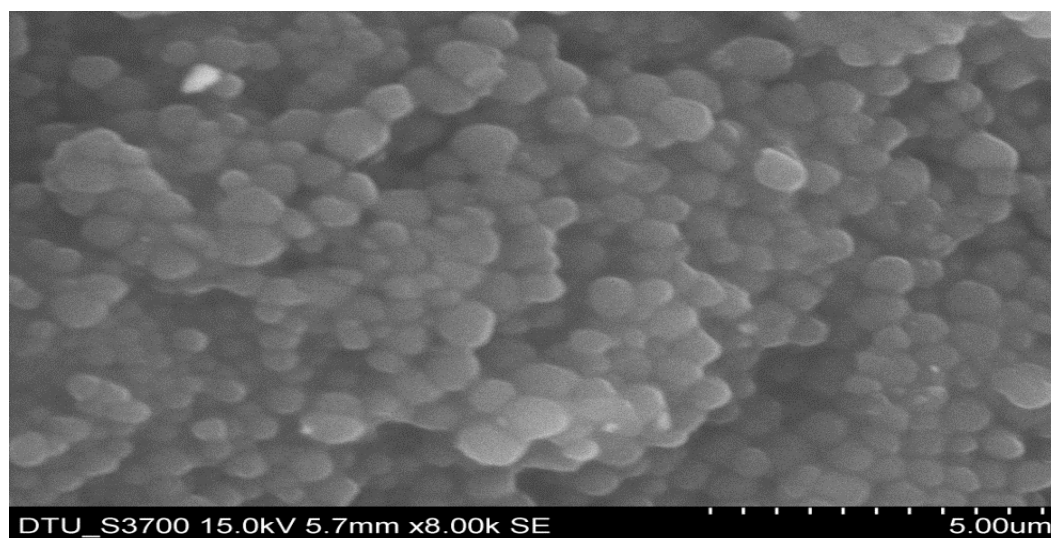


Fig. 4.28: SEM micrograph of F1-PANAm

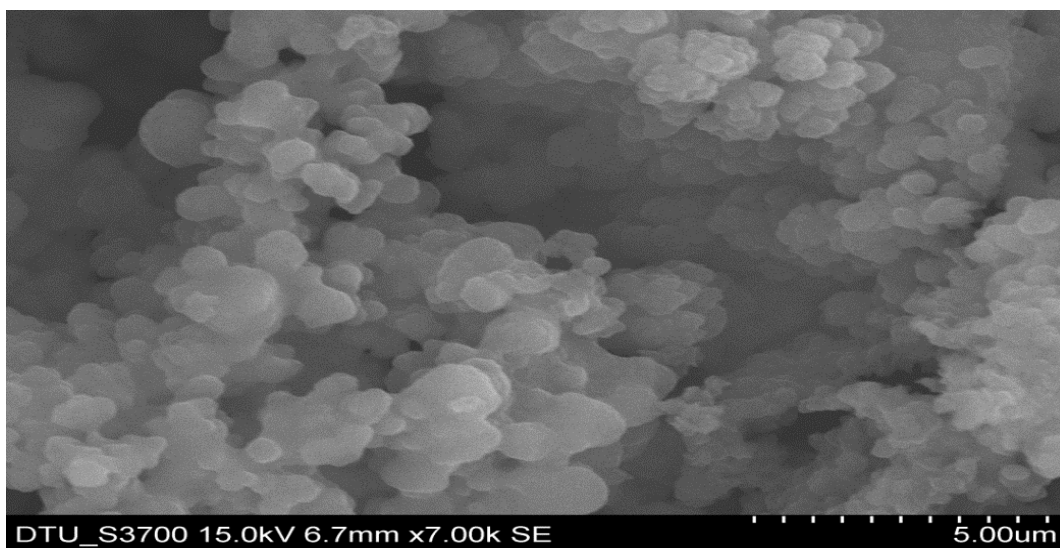


Fig. 4.29: SEM micrograph of F1-PANMA

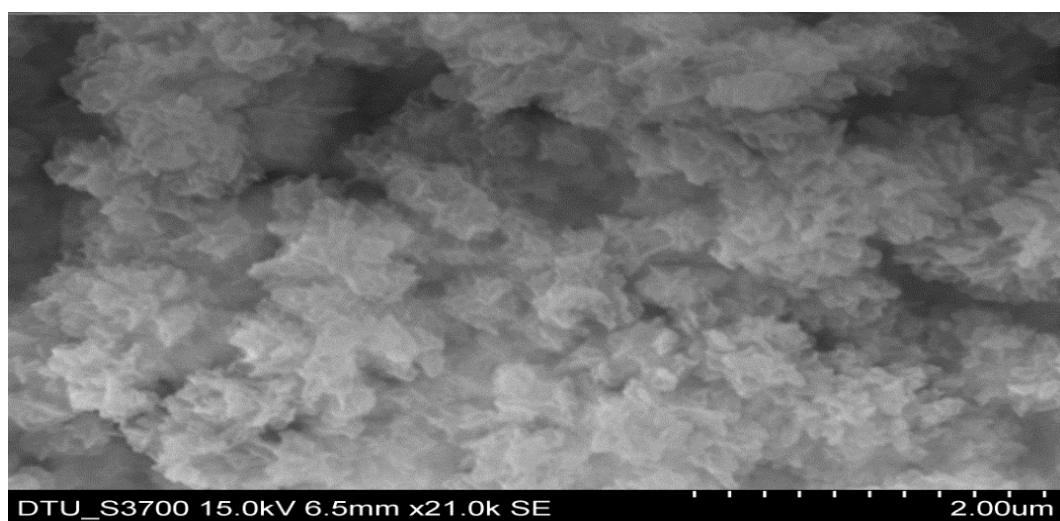


Fig. 4.30: SEM micrograph of F2-PAN

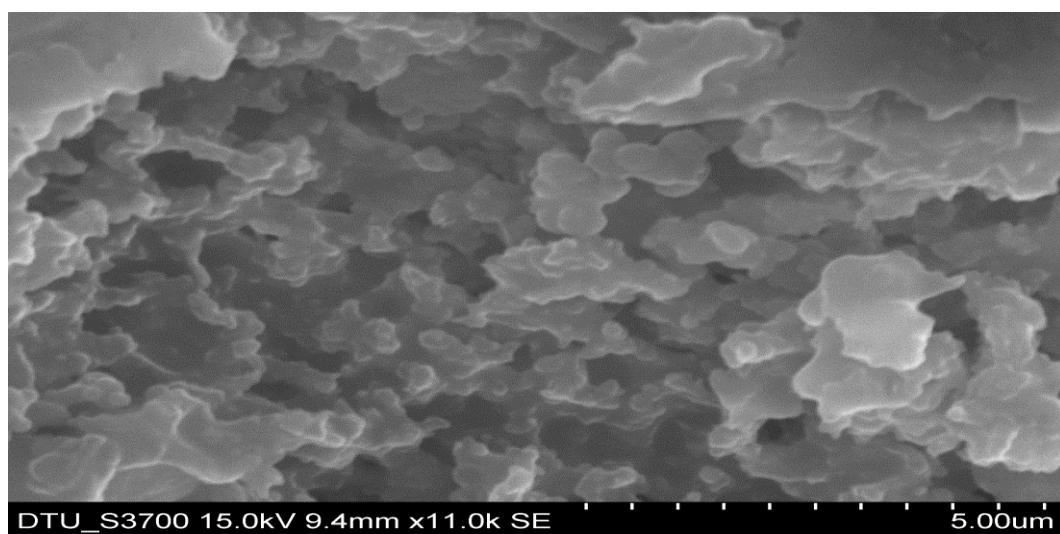


Fig. 4.31: SEM micrograph of F2-PANS

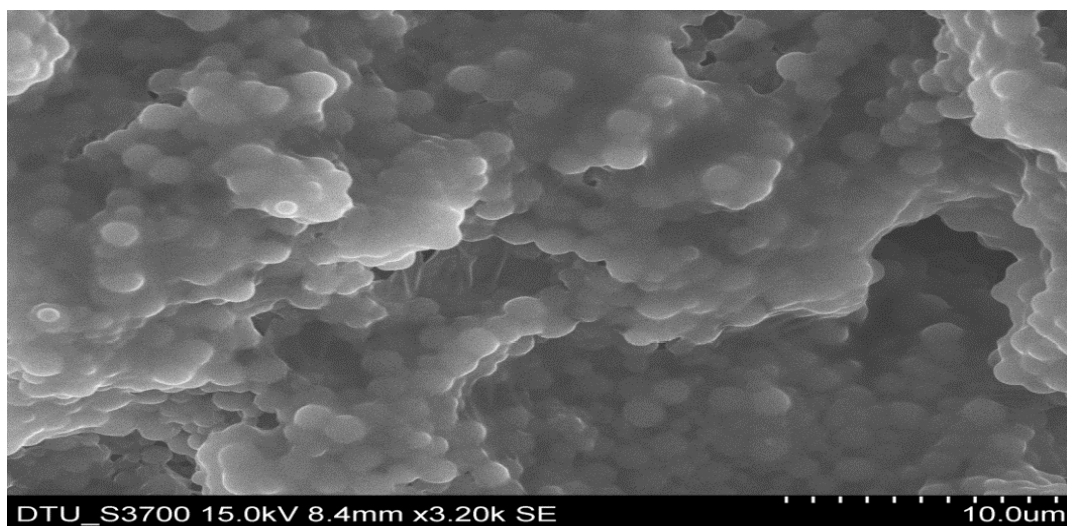


Fig. 4.32: SEM micrograph of F2-PANAm

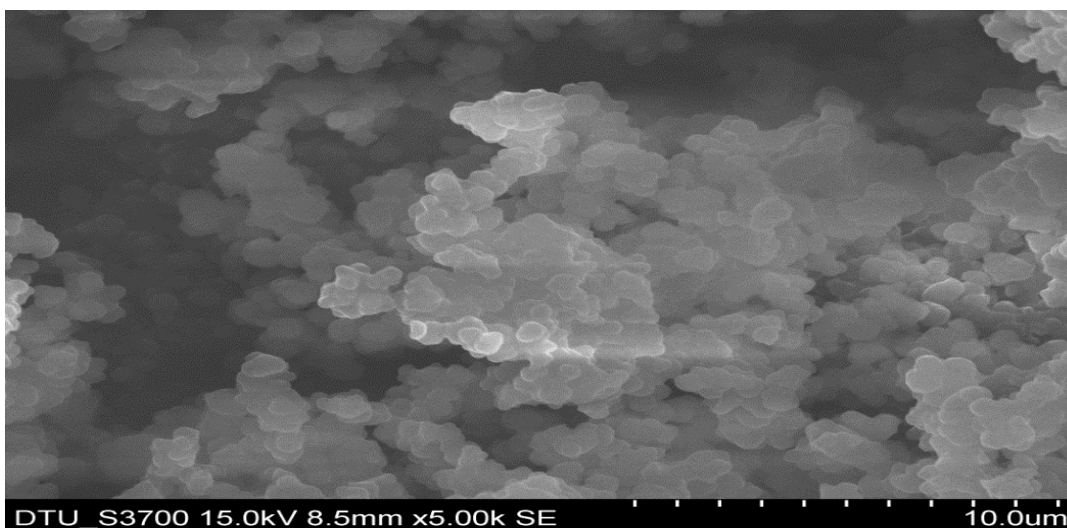


Fig. 4.33: SEM micrograph of F2-PANMA

As seen from the above SEM micrographs, we can conclude that resins with large number of pores can adsorb large amount of metal ions. F2-PANS and F2-PANMA resins have large number of pores as we can see from the SEM micrographs (fig 4.31 and 4.33) and these two resins adsorbed a large amount of metal ions.

4.5 Thermogravimetric Analysis

The thermal properties of polymer resins were evaluated using TGA. Functionalized PAN possesses good thermal stability and effect of copolymerization and functionalization on its

thermal stability was studied using TGA. The TGA thermogram of resins shows that F2-PAN is completely stable up to a temperature of 130 °C and it started losing weight above this temperature at a slow rate. At this rate, it degraded to 90 % of its initial weight. Above 350 °C, the degradation become rapid and it lost all its weight at around 510 °C.

The TGA thermograms of the functionalized polymer resin F2-PANS (fig. 4.35), F2-PANAm (fig. 4.36) and F2-PANMA (fig. 4.37) are also similar to that of TGA thermogram of the F2-PAN (fig. 4.34). They are all stable up to a temperature of 125 °C and above this temperature they start losing weight at slow rate. At a temperature around 330-350 °C, their degradation become rapid, and all of them are completely degraded at around 450 °C.

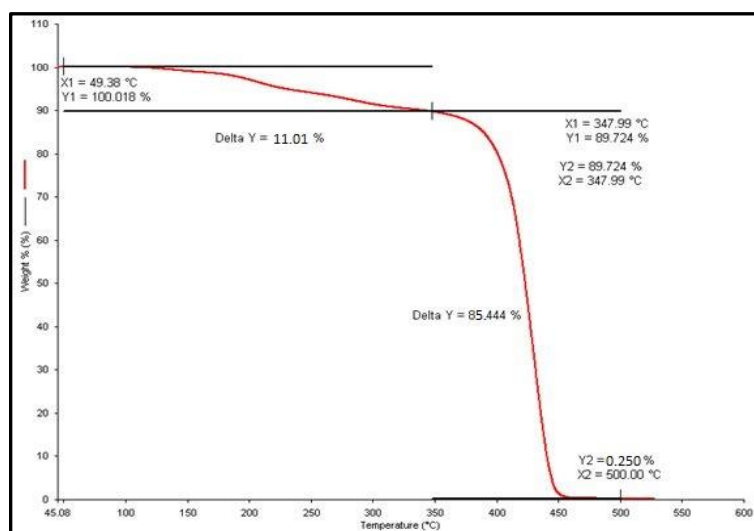


Fig. 4.34: TGA thermogram of F2-PAN

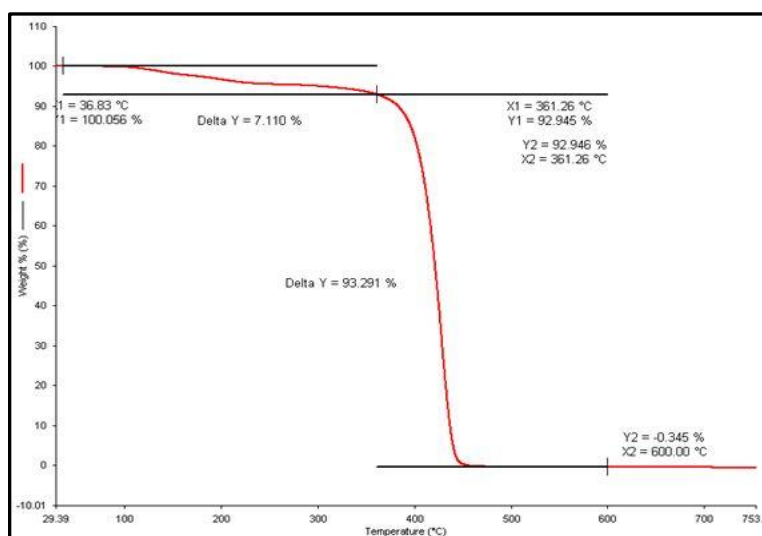


Fig. 4.35: TGA thermogram of F2-PANS

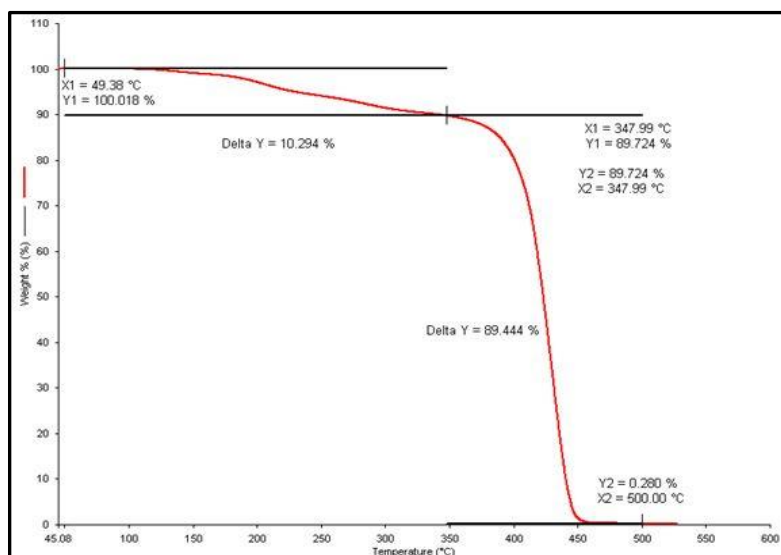


Fig. 4.36: TGA thermogram of F2-PANAm

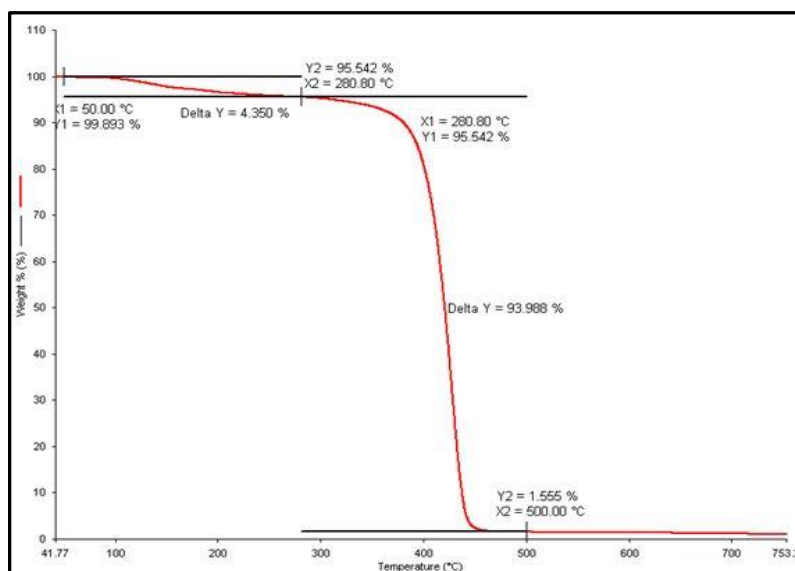


Fig. 4.37: TGA thermogram of F2-PANMA

In the light of above TGA data, we can conclude that there is no noticeable change in the thermal stability of the resins upto 400 °C.

4.6 DSC Analysis:

The DSC was used for the thermal analysis of the functionalized PAN and its copolymers. The DSC thermogram of F2-PAN (fig. 4.38) shows that the glass transition temperature of F2-PAN is around 100 °C. A large peak at 260 °C is probably because of the crystallization due to the

alignment of polymeric chains. The glass transition values of F2-PANS (fig. 4.39), F2-PANAm (fig. 4.40) and F2-PANMA (fig. 4.41) obtained from the DSC studies are around 110, 105 and 140 °C. In the DSC thermogram of F2-PANS, F2-PANAm and F2-PANMA, the exothermic peaks at around 250, 210 and 310 °C show the crystallization. Also the peaks at around 350 and 300 °C probably represent the cross-linking of the functionalized copolymer resins in the DSC thermogram of F2-PANS and F2-PANAm, respectively.

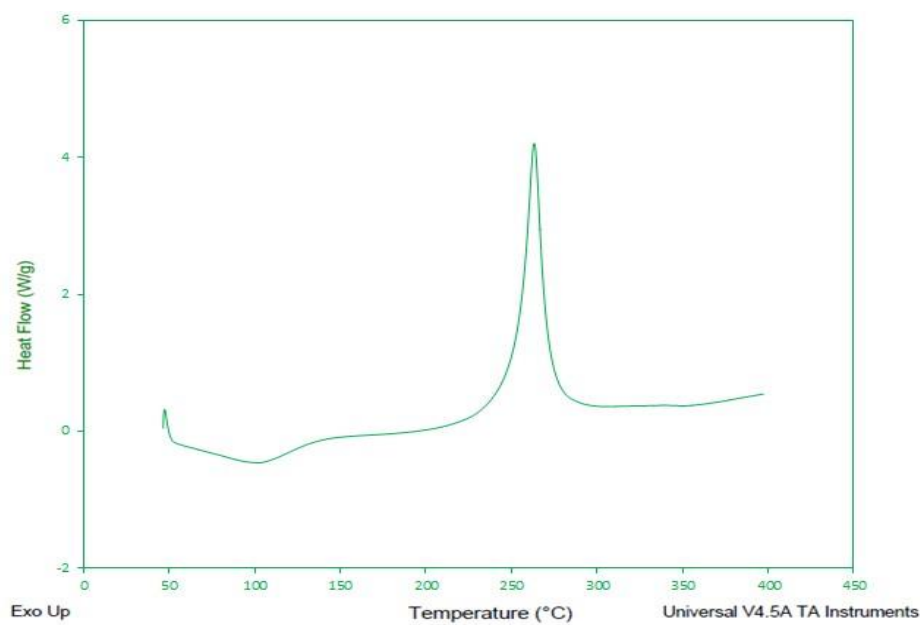


Fig. 4.38: Heat flow v/s Temperature graph of F2-PAN

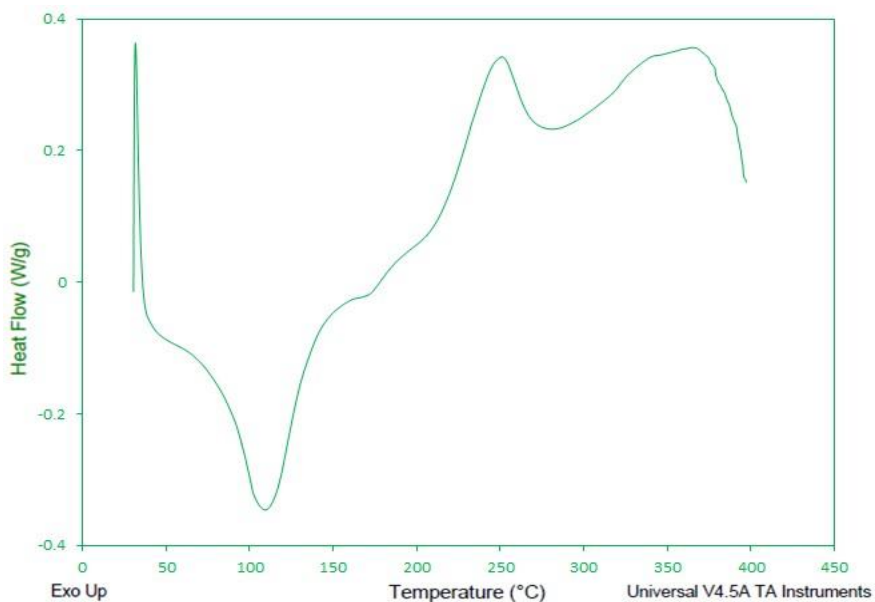


Fig. 4.39: Heat flow v/s Temperature graph of F2-PANS

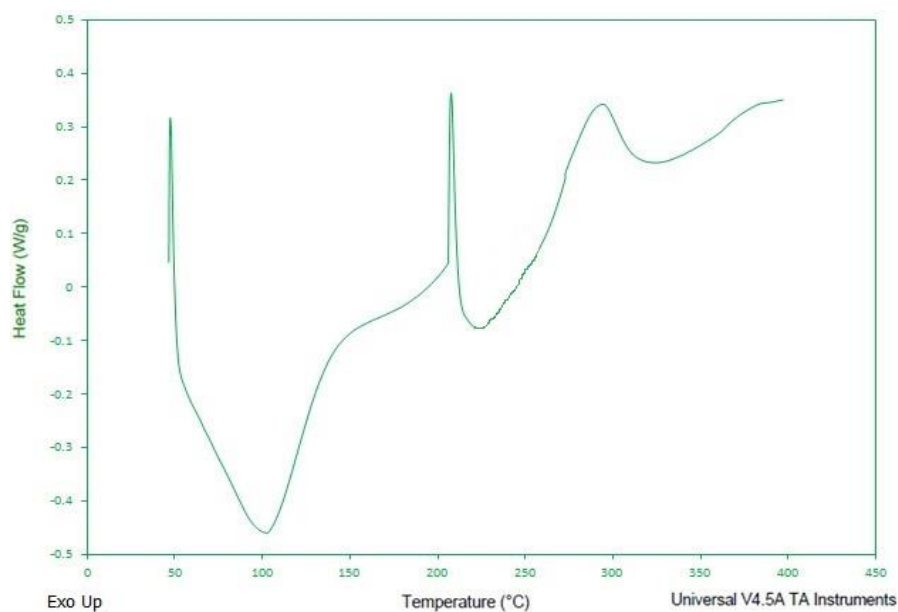


Fig. 4.40: Heat flow v/s Temperature graph of F2-PANAm

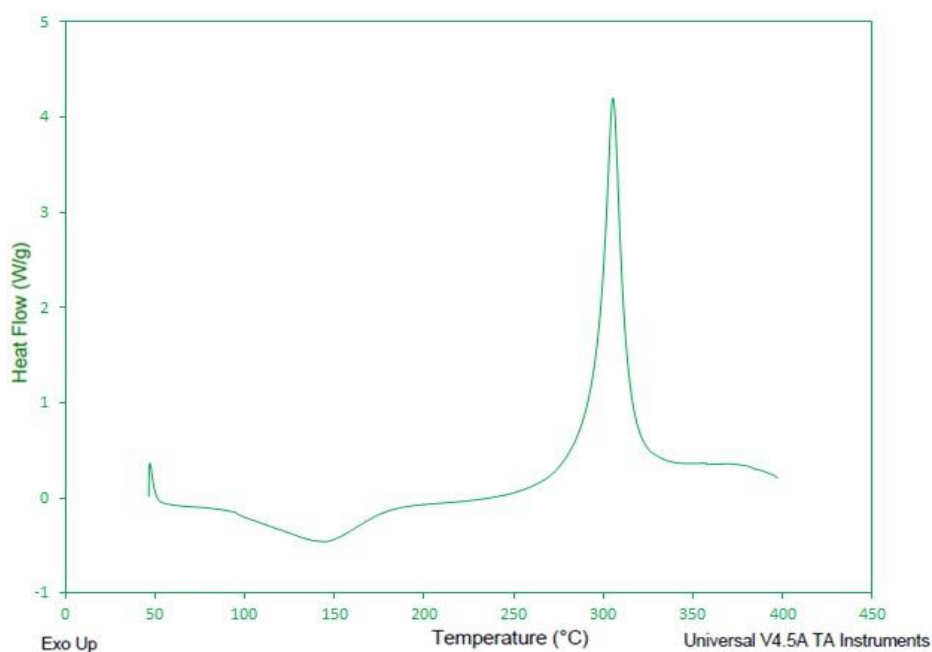


Fig. 4.41: Heat flow v/s Temperature graph of F2-PANMA

From the DSC thermogram of resins, we can conclude that on increasing the functional groups in the copolymer resins, T_g of the resins also increases. There is also increase in cross-linking of the copolymer resins.

4.7 Dynamic Mechanical Analysis:

DMA was also used to observe the effect of copolymerization. The glass transition temperature of F2-PAN obtained from DMA results is 85.3 °C. The DMA graph of the F2-PAN (fig. 4.42) shows that the functionalization has negligible effect on the glass transition temperature of PAN homopolymer. Glass transition temperature of polystyrene is less than that of PAN and copolymerization of acrylonitrile with styrene should result in a decrease in the glass transition temperature of the copolymer. The DMA graph of the F2-PANS (fig. 4.43) also supports this. The glass transition temperature is found to be 83.5 °C for F2-PANS and it is less than that of F2-PAN.

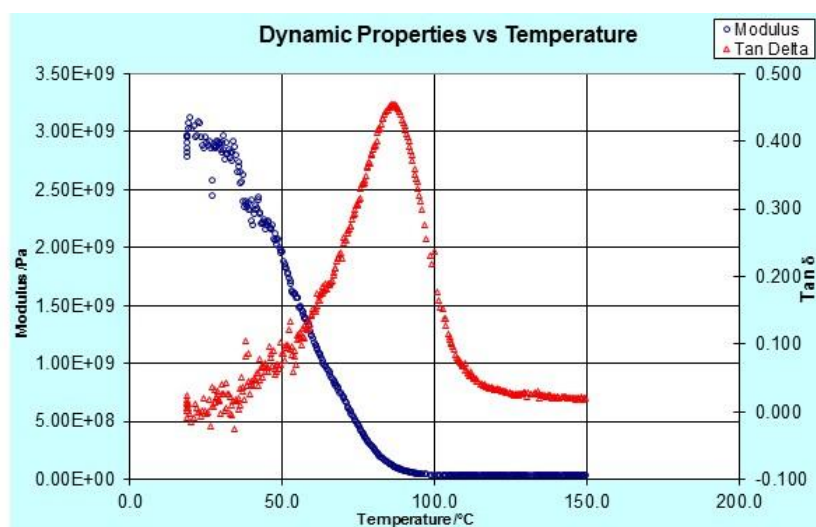


Fig. 4.42: Dynamic properties v/s Temperature graph of F2-PAN

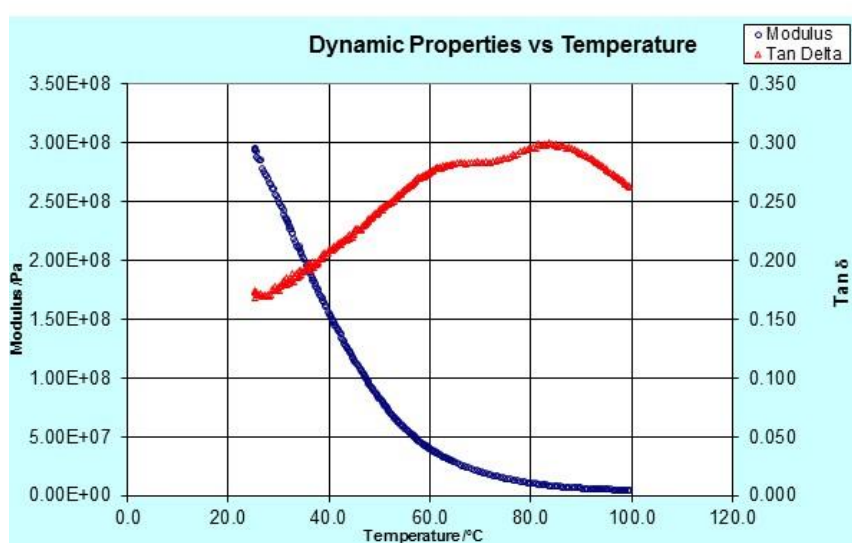


Fig. 4.43: Dynamic properties v/s Temperature graph of F2-PANS

The use of acrylamide as comonomer results in an increase in the glass transition temperature of F2-PANAm. The glass transition temperature of F2-PANAm is 86 °C as obtained from the DMA graph (fig. 4.44). Only a slight increase in the glass transition temperature is recorded. The F2-PANMA (fig. 4.45) registered the highest glass transition temperature of 106.8 °C which is significantly higher than the glass transition temperature of other copolymers.

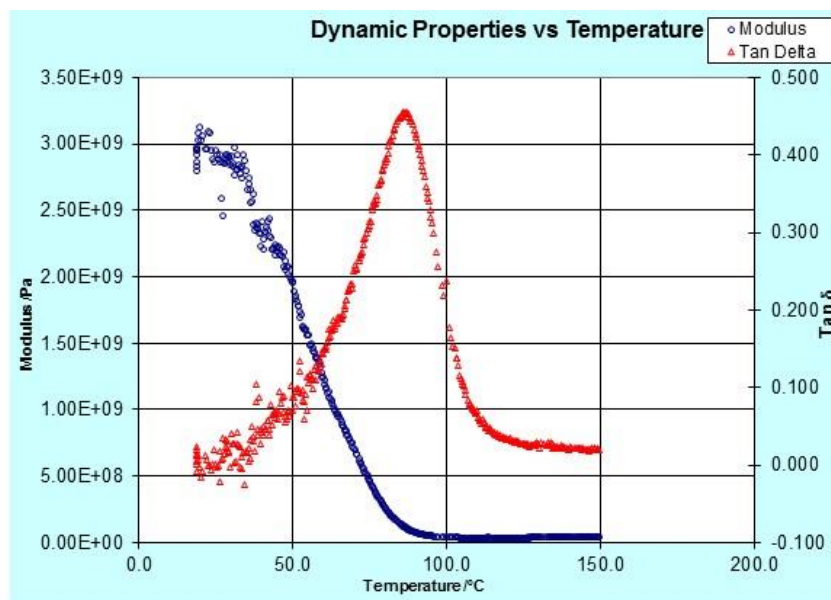


Fig. 4.44: Dynamic properties v/s Temperature graph of F2-PANAm

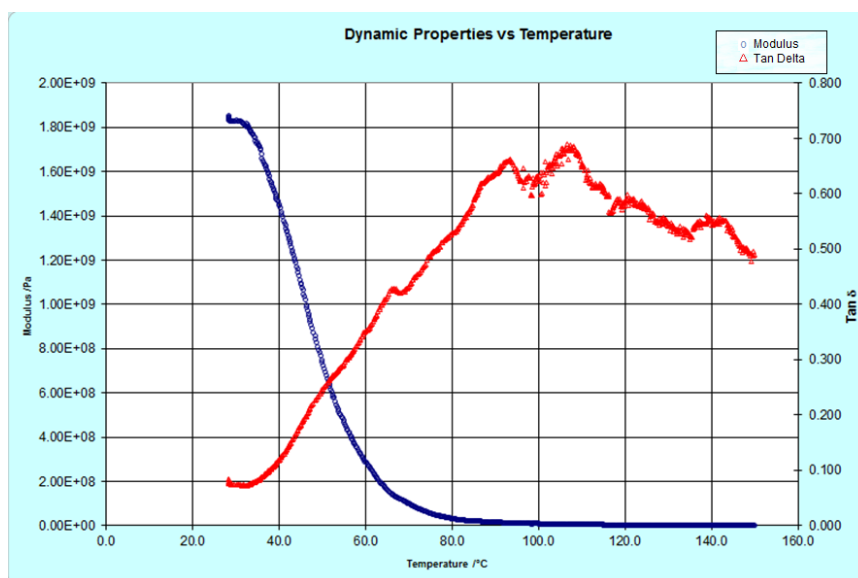


Fig. 4.45: Dynamic properties v/s Temperature graph of F2-PANMA

In the light of DMA results, we can conclude that there is no adverse effect of copolymerization on the glass transition temperature of the resins. An increase in the functional groups, T_g of the resins also increases.

CHAPTER-5

CONCLUSION

In the present work, synthesis and characterization of functionalized polyacrylonitrile and its copolymer resins were done for the adsorption of Hg^{2+} and Fe^{2+} from aqueous solution. Copolymer resins of acrylonitrile with styrene, acrylamide and methacrylic acid were prepared and functionalized using two ratios of resin and TETA (1:10 and 1:15). FTIR data show the introduction of $\text{C}=\text{O}$, $=\text{N}-\text{H}$ and $\text{C}=\text{NH}$ group in copolymer resins after functionalization. The EDS results revealed that F2-PANS have highest adsorption capacity for Hg^{2+} and F2-PANMA for Fe^{2+} . According to EDS studies, F2-PANS has 86.39 Weight % of Hg^{2+} and F2-PANMA has 87.47 weight % of Fe^{2+} . SEM analysis shows that these two resins are highly porous and these pores are probably responsible for higher adsorption. Both F2-PANS and F2-PANMA were functionalized using higher ratio of resin to TETA (1:15) which imply that amount of adsorption increased with increase in the amount of TETA used for functionalization. It is also found that the copolymerization and functionalization did not affect the thermal stability of copolymer resins as shown by the TGA results. The glass transition temperature of F2-PANMA is highest as indicated by DMA. This is also supported by the DSC studies. Therefore these copolymer resins can be used for the adsorption of Hg^{2+} and Fe^{2+} from their aqueous solution. The average molecular weight of polymer and its copolymers samples was also determined by using Ostwald viscometer and found to be 130606, 150304, 157022 and 167233, respectively. The results of viscometric analysis show that the average molecular weight of PAN based copolymer resins is higher than the PAN resin and poly(acrylonitrile-methacrylic acid) copolymer resin has highest value of molecular weight than the other PAN and its copolymer resins.

CHAPTER-6

FUTURE PROSPECTS

Today water pollution is one of the major threats for the whole world. Scientists are paying a lot of attention to develop techniques for the removal of toxic substances from water and purification. Intake of Metals such as mercury in excess can be lethal to human body. The polymer resin prepared in the present work can be used to remove metals such as mercury and iron from industrial aqueous discharges. By modifying the copolymer resins, it can be used for a wide range of pH and temperature. These copolymers has the potential to be used as membrane for the filters and by suitably modifying it, it can be used at industrial scale for the treatment of polluted water.

REFERENCES

- 1) N. Arsalani, E. Ghasemi, R. Rakh, A. A. Entezami, Synthesis and application of chelating resins based on polyacrylonitrile diethylenetriamine for metal ions removal, J. Iran. Chem. Res. 3 (2010) 195-204.
- 2) J.A. Brydson, *Plastics Materials*, seventh edition, ISBN 0 75064132 0.
- 3) Stanley R. Sandler, Wolf Karo, Jo-Anne Bonesteel and Eli M. Pearce, *Polymer Synthesis and Characterization*, ISBN: 978-0-12-618240-8.
- 4) <http://www.britannica.com/EBchecked/topic/468259/polyacrylonitrile-PAN>.
- 5) <http://www.pslc.ws/macrog/pan.htm>.
- 6) www.sciencedirect.com
- 7) G.R. Kiani, H. Sheikhoie, N. Arsalani, Heavy metal ion removal from aqueous solutions by functionalized Polyacrylonitrile, *Desalination* 269 (2011) 266–270.
- 8) Y. Chen, Y. Zhao, Synthesis and characterization of polyacrylonitrile-2-amino-2-thiazoline resin and its sorption behaviours for noble metal ions, *Reactive & Functional Polymers* 55 (2003) 89–98.
- 9) T. Chaisuwan, T. Komalwanich, S. Luangsukrerk, S. Wongkasemjit, Removal of heavy metals from model wastewater by using polybenzoxazine aerogel, *Desalination* 256 (2010) 108–114.
- 10) M. H. E. Newehy, A. Alamri, S. S. Al-Deyab, Optimization of amine-terminated Polyacrylonitrile synthesis and characterization, *Arabian Journal of Chemistry* (2014) 7, 235–241.
- 11) C. Klaysom, S. Hermans, A. Gahlaut, S. V. Craenenbroeck, Ivo F.J. Vankelecom, Polyamide/Polyacrylonitrile (PA/PAN) thin film composite osmosis membranes: Film optimization, characterization and performance evaluation, *Journal of Membrane Science* 445 (2013) 25–33.
- 12) A. Dastbaza, A. Reza. Keshtkar, Adsorption of Th^{4+} , U^{6+} , Cd^{2+} , and Ni^{2+} from aqueous solution by a novel modified polyacrylonitrile composite nanofiber adsorbent prepared by electrospinning, *Applied Surface Science* 293 (2014) 336–344.
- 13) B. L. Rivas Ivan, M. Peric, S. Villegas, Synthesis and metal ion uptake properties of water-insoluble functional copolymers: removal of metal ions with environmental impact, *Polymer. Bull.* (2010) 65:917–928.
- 14) <http://www.colby.edu/chemistry/PChem/lab/DiffScanningCal.pdf>.

- 15) A. Razik H.H., Azza M., E.Asma, Abbo M, Heavy metal adsorbents based on chelating amidoximated grafted cellulose. International Journal of Basic and Applied Chemical Sciences ISSN: 2277-2073.
- 16) A. Nilchia, R. Saberla, M. Moradib, H. Azizpourb, R. Zarghami, Adsorption of cesium on copper hexacyanoferrate–PAN composite ion exchanger from aqueous solution, Chemical Engineering Journal 172 (2011) 572–580.
- 17) M. A. A. Zainia, Y. Amanoa, M. Machidaa, Adsorption of heavy metals onto activated carbons derived from polyacrylonitrile fiber, Journal of Hazardous Materials 180 (2010) 552–56.
- 18) A. Nilchia, R. Saberla, S. R. Garmarodia, A. Bagheria, Evaluation of PAN-based manganese dioxide composite for the sorptive removal of cesium-137 from aqueous solutions, Applied Radiation and Isotopes 70 (2012) 369–374.
- 19) P. K. Neghlani, M. Rafizadeh, F. A. Taromi, Preparation of aminated-polyacrylonitrile nanofiber membranes for the adsorption of metal ions: Comparison with microfibers, Journal of Hazardous Materials 186 (2011) 182–189.
- 20) F. Jia, C. Lia, B. Tanga, J. Xua, G. Lub, P. Liua, Preparation of cellulose acetate/zeolite composite fiber and its adsorption behavior for heavy metal ions in aqueous solution, Chemical Engineering Journal 209 (2012) 325–333.